

THE MEASUREMENT OF PHOTOGRAPHIC IMAGES BY HUMAN OPERATORS

NGA review(s) completed.

25X1

THE MEASUREMENT OF PHOTOGRAPHIC IMAGES BY HUMAN OPERATORS

March 17, 1967

25X1

ACKNOWLEDGEMENTS

5X1 The assistance given the authors by [] is very much appreciated. He conducted the experimental sessions and worked with the N computer facility in obtaining the initial computations. His efforts contributed significantly to the success of the experiment.

25X1

The authors wish also to thank each of the staff members of the T Branch who spent many hours serving as subjects in the experiment. Their willingness to assist and their cooperation is gratefully acknowledged.

TABLE OF CONTENTS

	Page
ACKNOWLEDGEMENTS	iii
LIST OF TABLES AND FIGURES	vii
Chapter	
I SUMMARY	1
II INTRODUCTION	5
III METHOD	7
EXPERIMENTAL VARIABLES	7
LAYOUT OF GEOMETRIC SHAPES	8
MASTER PLATE	11
GEMS	11
SUBJECTS AND EQUIPMENT	13
EXPERIMENTAL DESIGN AND PROCEDURE	14
INSTRUCTIONS	14
COMPUTATION OF POSITIONING ERRORS	16
IV ANALYSES AND RESULTS	17
THE PRECISION OF POINTING ON THE MASTER PLATE	17
PRELIMINARY ANALYSES OF THE POINTING ERRORS FOR EDGES ON THE GEMS	18
<u>Means of the Pointing Errors</u>	19
<u>Standard Deviations of the Pointing Errors</u>	20
<u>Combination of Variables Within Gems</u>	21
THE EFFECTS OF THE EDGE SPREAD, MODULATION, SHAPE, AND POLARITY OF THE EDGE ON THE MEANS AND THE STANDARD DEVIATIONS OF THE POINTING ERRORS	22
<u>Means of the Pointing Errors</u>	22
<u>Standard Deviations of Pointing Errors</u>	23
<u>Operator Errors in Measuring the Extent of Images</u>	26
THE MEASUREMENT OF BAR WIDTHS	27
<u>Preliminary Analyses--Mean of Measurement Errors</u>	27
<u>Preliminary Analyses--Standard Deviations of Measurement Errors</u>	28

TABLE OF CONTENTS (cont.)

Chapter	Page
<u>Means and Standard Deviations of</u> <u>Measurement Errors</u>	28
V DISCUSSION AND APPLICATION OF RESULTS.	31
QUALIFICATION OF THE RESULTS.	31
ATTEMPTS TO RELATE ACTUAL EDGE POSITIONS WITH POINTING ERRORS	31
THE RELATIVE CONTRIBUTIONS OF EDGE SPREAD AND MODULATION TO MEASUREMENT	32
APPLICATION OF RESULTS.	32
APPENDIX A	
THE COMPUTATION OF THE MEAN AND THE STANDARD DEVIATION OF MEASUREMENT ERRORS	33
<u>The Mean of Measurement Errors</u>	33
<u>The Standard Deviation of Measurement</u> <u>Errors</u>	34
APPENDIX B	
PREPARATION OF THE STIMULI.	45

LIST OF TABLES AND FIGURES

Table		Page
1	THE VALUES OF EDGE SPREAD AND MODULATION INVESTIGATED	7
2	THE VALUES OF THE COMBINED EDGE SHAPES AND EDGE SIZES REPRESENTED IN EACH GEM.	8
3	THE DESCRIPTION AND THE NUMBERS OF THE EDGES . .	9
4	AVERAGE STANDARD DEVIATIONS (IN MICRONS) OF THE X-COORDINATE VALUES FOR THE FIDUCIALS, STRAIGHT AND CURVED EDGES ON THE MASTER PLATE	18
5	STANDARD DEVIATIONS (IN MICRONS) OF THE X-COORDINATE VALUES FOR THE POINTED EDGES ON THE MASTER PLATE	18
6	AVERAGE STANDARD DEVIATIONS IN MICRONS OF MEASUREMENT ERRORS FOR THE FIVE EDGE SPREADS AND FOR .10 MODULATION AND FOR .15 TO .50 MODULATIONS COMBINED	29
1A	MEAN POINTING ERROR (IN MICRONS) FOR THE DIFFERENT EDGE SHAPES AND THE TWO POLARITIES AT EACH EDGE SPREAD. ALL MODULATIONS COMBINED	33
2A	EDGE SPREAD-5.0 MICRONS. MODULATION-.10	35
3A	EDGE SPREAD-7.5 MICRONS. MODULATION-.10	35
4A	EDGE SPREAD-11.2 MICRONS. MODULATION-.10	36
5A	EDGE SPREAD-16.8 MICRONS. MODULATION-.10	36
6A	EDGE SPREAD-7.5 MICRONS. MODULATION-.15	36
7A	EDGE SPREAD-24.0 MICRONS. MODULATION-.15	37
8A	EDGE SPREAD-7.5 MICRONS. MODULATION-.22	37
9A	EDGE SPREAD-11.2 MICRONS. MODULATION-.22	37
10A	EDGE SPREAD-16.8 MICRONS. MODULATION-.22	38
11A	EDGE SPREAD-24.0 MICRONS. MODULATION-.22	38
12A	EDGE SPREAD-5.0 MICRONS. MODULATION-.33	38

LIST OF TABLES AND FIGURES (cont.)

Table		Page
13A	EDGE SPREAD-7.5 MICRONS. MODULATION-.33	39
14A	EDGE SPREAD-11.2 MICRONS. MODULATION-.33 . . .	39
15A	EDGE SPREAD-16 MICRONS. MODULATION-.33	39
16A	EDGE SPREAD-24.0 MICRONS. MODULATION-.33 . . .	40
17A	EDGE SPREAD-5.0 MICRONS. MODULATION-.50	40
18A	EDGE SPREAD-7.5 MICRONS. MODULATION-.50	40
19A	EDGE SPREAD-11.2 MICRONS. MODULATION-.50 . . .	41
20A	EDGE SPREAD-25.0 MICRONS. MODULATION-.50 . . .	41
 Figure		
1	The layout of the geometric shapes	10
2	Planned (closed points) and obtained (opened points) modulation and edge spread values for each Gem	11
3	Edge gradients of the Gems	12
4	Superimposition of three microdensitometer traces and the method used to measure and describe the edge spread and the modulation	12
5	Mann 621 Comparator, center. Data translator (right) and IBM card puncher (left).	13
6	Mean pointing error for polarity-A edges as a function of edge spread. All modulations combined	22
7	Mean pointing error for polarity-B edges as a function of edge spread. All modulations combined	22
8	Standard deviations of the pointing errors for polarity-A curved edges as a function of modulation and edge spread	24

LIST OF TABLES AND FIGURES (cont.)

Figure		Page
9	Standard deviations of the pointing errors for polarity-A 135° angles as a function of modulation and edge spread	24
10	Standard deviations of the pointing errors for polarity-A 90° angles as a function of modulation and edge spread	24
11	Standard deviations of the pointing errors for polarity-A 45° angles as a function of modulation and edge spread	24
12	Standard deviations of the pointing errors for polarity-A 22° angles as a function of modulation and edge spread	25
13	Standard deviations of the pointing errors for polarity-B curved/straight edges as a function of modulation and edge spread.	25
14	Standard deviations of the pointing errors for polarity-B 135° angles as a function of modulation and edge spread	25
15	Standard deviations of the pointing errors for polarity-B 90° angles as a function of modulation and edge spread	25
16	Standard deviations of the pointing errors for polarity-B 45° angles as a function of modulation and edge spread	26
17	Standard deviations of the pointing errors for polarity-B 22° angles as a function of modulation and edge spread	26
18	Mean measurement error for low transmittance bars as a function of edge spread and bar width. All modulations combined	28
19	Mean measurement error for high transmittance bars as a function of edge spread and bar width. All modulations combined.	29

LIST OF TABLES AND FIGURES (cont.)

Figure		Page
1A	Examples of hypothetical images. The dot on the line shows the location of the mean error relative to the edge. The number above each line is the mean pointing error in microns	34
1B	Characteristic curves for Kodak Type 3404 film .	46
2B	Characteristic curves for Kodak Type 8430 film .	47
3B	Photomicrograph of Gem No. 12	47

Chapter I

SUMMARY

Many factors contribute to errors of mensuration of images in aerial photographs. Among them are uncertainties about the geometry of the photography due to a lack of knowledge of the exact camera position and camera pointing, and uncertainties of the focal length of the camera lens. Other sources of error are the dimensional instability of films (e.g., films may stretch or shrink), the operational characteristics of the measuring equipment, and the human operator of the equipment.

This study was concerned with only one source of mensuration error--the human operator. The primary purpose of the study was to determine human operators' measurement errors as a function of edge spread (resolution), modulation (contrast), image shape, and image size.

The edge spread ranged from 5 microns to 24 microns in five steps and the modulation ranged from 0.1 to 0.5 in five steps. The shapes and sizes of edges at each combination of edge spread and modulation were as follows:

STRAIGHT EDGES. There were three edge sizes--24, 48, and 96 microns.

CURVED EDGES. There were four curvatures defined by radii of 190, 96, 48, and 24 microns. There were three edge sizes for the 190-micron and 96-micron edges, two sizes for the 48-micron edge, and there was one size for the 24-micron edge. (See Table 2, pg. 8.)

POINTED EDGES. There were four pointed edges defined by angles of 22, 45, 90, and 135 degrees. There were three sizes, 24, 48, and 96 microns, for each of the four angles.

Each radius-size and angle-size combination represented two edges that differed from one another in the polarity of the densities forming the edge. That is, the left side of one edge was more dense than the right side; the reverse was true for the other edge. The images of the edges were spaced in the photographs so that the edge spread of one edge did not overlap that of another.

In addition to the edges described above, there were three dark (low transmittance) bars on a light (high transmittance) background and three light bars on a dark background. The bars in each set of three were 6, 12, and 24 microns wide. Unlike the images of the other edges, the bars were included to assess the effects of edge spread on measurement when there is some overlap of the edge spread of adjacent edges.

The subjects were six operators experienced at measuring photographic images. The images were measured using a Mann 621 Comparator. The subjects' task was to position a cross-hair on each edge.

Two measures were computed for each edge at each combination of edge spread and modulation. These were the mean of the positioning errors (accuracy) and the standard deviation of the positioning errors (precision) of the six operators. In addition a mean and standard deviation of measurements of the width of each bar was computed.

The results of the study were as follows:

ACCURACY: MEAN ERROR

1. There was no apparent relation between the accuracy of positioning and the modulation, size or curvature of the edge.
2. Accuracy of positioning decreased with an increase in edge spread.
3. Accuracy of positioning decreased with an increase in the acuteness of the pointed edges.
4. Accuracy of the measurement of the widths of bars decreased as the edge spread increased. Accuracy decreased by only a few microns for bar widths of 24 microns and by as much as 10 or 12 microns for bar widths of 6 microns.

PRECISION: DIFFERENCES AMONG OPERATORS

1. There was no apparent relation between the precision of positioning and the size or curvature of the edge.
2. The precision of positioning decreased with an increase in the edge spread.
3. The precision of positioning decreased with an increase in the acuteness of the pointed edges.

4. A change in modulation from .50 to .22 had no effect on the precision of positioning. Precision decreased only when the modulation was reduced to about .15 or .10--a modulation so low that the image was barely visible.

Chapter II

INTRODUCTION

Intelligence is usually extracted from aerial photography in two ways: photointerpretation and mensuration. In the opinion of intelligence analysts mensuration provides as much or more of the directly useful intelligence obtained from photography than does photointerpretation. Furthermore, measurements aid the photointerpreter in identifying targets and in distinguishing among targets of similar appearance. It was the recognition of this important role of mensuration that stimulated the undertaking of the experiment described here.

Many factors contribute to the errors of measurements made on aerial photographs. Among these factors are uncertainties about the geometry of the photography due to a lack of knowledge of the exact camera position and pointing, and uncertainties of the focal length of the camera lens. The dimensional instability of films (e.g., the film may stretch or shrink) and the operational characteristics of mensuration equipment can also contribute to errors.

The experiment reported here was concerned with yet another source of mensuration error, the human measuring the images. A computer program which contains inputs for several possible sources of mensuration error is under development at N _____; its purpose is to predict from these sources the probable error of mensuration. It was intended that the results of this experiment would provide the probable errors generated by the human operator.

The operators' measurement errors depend in large part on the characteristics of the photographic images being measured. Thus, the purpose of this experiment was to determine the accuracy and precision of measurement of photographic images as a function of the edge spread, modulation, shape, and size of the image.

Chapter III

METHOD

An extremely large variety of image characteristics (edge spread, modulation, shape, and size) is routinely encountered in mensuration and the inclusion of the universe of these characteristics in a single experiment would be impracticable. Consequently the stimulus materials for this experiment consisted of a sample of image characteristics. These characteristics were typical of those encountered in operational photography.

EXPERIMENTAL VARIABLES

The primary experimental variables were edge spread (equivalent to a resolution range from 20 to 200 cycles per millimeter) and modulation (equivalent to a contrast range from 1.2/1 to 3/1).¹ The values of edge spread and modulation investigated are shown in Table 1. Each numbered cell in the table represents a photograph having a unique combination of values of edge spread and modulation.² Photographs such as these, which have specific image-structure characteristics, are called "Gems." The numbers in Table 1 identify the Gems. The circled numbers represent six Gems not used in the experiment. Gem 5 was omitted because the images were extremely difficult to see. The remaining five Gems (6, 8, 9, 11, 24) were omitted because of a limitation upon the time available for the performance of the experiment.

TABLE 1
THE VALUES OF EDGE SPREAD
AND MODULATION INVESTIGATED.

		EDGE SPREAD* (MICRONS)				
		5.0	7.5	11.2	16.8	24.0
MODULATION*	.50	21	22	23	24	25
	.33	16	17	18	19	20
	.22	11	12	13	14	15
	.15	6	7	8	9	10
	.10	1	2	3	4	5

*APPROXIMATE VALUES

In addition to the variation of edge spread and modulation among Gems, edge shape and edge size were varied within each Gem.

¹ An approximation formula for converting edge spread to resolution is:

$$\frac{1}{\text{edge spread (mm)}} = \text{resolution (c/mm)}.$$

The formula for converting modulation to contrast is:

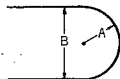
$$\frac{1 + \text{modulation}}{1 - \text{modulation}} = \text{contrast}.$$

² These tabled values are those planned but not precisely produced. The values produced are shown later in Figure 2. For the purposes of this experiment the differences were considered trivial.

TABLE 2
THE VALUES OF THE COMBINED EDGE SHAPES
AND EDGE SIZES REPRESENTED IN EACH GEM

	EDGE SIZE (IN MICRONS)	POINTED EDGES (ANGLE-IN DEGREES)				CURVED EDGES (RADIUS-IN MICRONS)				STRAIGHT EDGES (RECTANGLES)
		22	45	90	135	24	48	96	190	
	48									
	96					--*				
	190					--*	--*			

*THESE SIZE-SHAPE COMBINATIONS ARE NOT POSSIBLE BECAUSE THE EDGE SIZES EXCEED THE RADII. FOR EXAMPLE:



EDGE SIZE "B" CANNOT BE GREATER THAN 2A.

Table 2 shows the different combinations of edge shape and edge size represented in each Gem. With the exception of the three cells containing dashes (these three combinations were not possible) and those appearing in the column labeled "straight edges," each cell represents two edges, both identical in size and shape but differing from one another in the polarity of the densities forming the edges. That is; the left side of one edge was more dense than the right side; the reverse was true for the other edge.

In addition to the edges described in Table 2, there were three dark bars (low transmittance) on a light (high transmittance) background and three light bars on a dark background. The bars in each set of three were 6, 12 and 24 microns wide. Unlike the other images, the bars were included to assess the effects of edge spread on the accuracy and the precision of measurement when there is some overlap of the edge spread of adjacent edges.

LAYOUT OF GEOMETRIC SHAPES

Simple geometric image shapes were used as stimuli. The images and their arrangement are shown in Figure 1. The numbers given in Figure 1 correspond to the individual fiducial marks and edges described in Table 3. Each image was of uniform density, and this density was less³ than the uniform density of the background. The X and Y coordinates of each mensuration point differed from those of any other, the exceptions being the Y coordinates of the edges of the six vertical bars. Except for the six bars the separation between image edges was at least twice the maximum edge spread so that the blur of one edge never overlapped that of another.

³ The only exception was the vertical bars formed by edges 11 to 16. The density of these bars was greater than the uniform density of their background.

TABLE 3

THE DESCRIPTION AND THE NUMBERS OF THE EDGES

IMAGE	FIDUCIAL OR EDGES	EDGE DESCRIPTION
FIDUCIAL MARKS	1.	BOTTOM LEFT OUTSIDE FIDUCIAL MARK
	2.	TOP LEFT " " "
	3.	TOP RIGHT " " "
	4.	BOTTOM RIGHT " " "
BARS	5.	RIGHT SIDE OF HIGH TRANSMITTANCE BAR 24μ WIDE
	6.	LEFT " " " 24μ " "
	7.	RIGHT " " " 12μ " "
	8.	LEFT " " " 12μ " "
	9.	RIGHT " " " 6μ " "
	10.	LEFT " " " 6μ " "
	11.	RIGHT " " LOW 24μ " "
	12.	LEFT " " " 24μ " "
	13.	RIGHT " " " 12μ " "
	14.	LEFT " " " 12μ " "
	15.	RIGHT " " " 6μ " "
	16.	LEFT " " " 6μ " "
POINTS	17.	HIGH TRANSMITTANCE 135° ANGLE, POINTED FIGURE 190μ WIDE
	18.	LOW " 135° " " 190μ "
	19.	HIGH " 90° " " 96μ "
	20.	LOW " 90° " " 96μ "
	21.	HIGH " 90° " " 48μ "
	22.	LOW " 90° " " 48μ "
	23.	HIGH " 45° " " 48μ "
	24.	LOW " 45° " " 48μ "
	25.	HIGH " 22° " " 48μ "
	26.	LOW " 22° " " 48μ "
	27.	HIGH " 135° " " 96μ "
	28.	LOW " 135° " " 96μ "
	29.	HIGH " 135° " " 48μ "
	30.	LOW " 135° " " 48μ "
	31.	HIGH " 45° " " 96μ "
	32.	LOW " 45° " " 96μ "
	33.	HIGH " 22° " " 96μ "
	34.	LOW " 22° " " 96μ "
	35.	HIGH " 90° " " 190μ "
	36.	LOW " 90° " " 190μ "
	37.	HIGH " 45° " " 190μ "
	38.	LOW " 45° " " 190μ "
	39.	HIGH " 22° " " 190μ "
	40.	LOW " 22° " " 190μ "
CURVED EDGES	41.	HIGH TRANSMITTANCE 96μ RADIUS, CURVED FIGURE 48μ WIDE
	42.	LOW " 96μ " " 48μ "
	43.	HIGH " 48μ " " 48μ "
	44.	LOW " 48μ " " 48μ "
	45.	HIGH " 190μ " " 190μ "
	46.	LOW " 190μ " " 190μ "
	47.	HIGH " 96μ " " 190μ "
	48.	LOW " 96μ " " 190μ "
	49.	HIGH " 190μ " " 48μ "
	50.	LOW " 190μ " " 48μ "
	51.	HIGH " 190μ " " 96μ "
	52.	LOW " 190μ " " 96μ "
	53.	HIGH " 96μ " " 96μ "
	54.	LOW " 96μ " " 96μ "
	55.	HIGH " 48μ " " 96μ "
	56.	LOW " 48μ " " 96μ "
	57.	HIGH " 24μ " " 48μ "
	58.	LOW " 24μ " " 48μ "
STRAIGHT EDGES	59.	STRAIGHT EDGE, 48μ LONG; FIGURE 48μ WIDE
	60.	" " 96μ " 48μ "
	61.	" " 190μ " 48μ "

The three bars formed by edges 5 and 6, 7 and 8, and 9 and 10 were identical to the three bars formed by edges 11 through 16, though they had opposite polarities. In addition, each edge was present in both polarities. The odd-numbered edges of the series 17 through 58 were of one polarity; hereafter these edges will be referred to as "polarity-A" edges. The even-numbered edges were of the other polarity which are hereafter referred to as "polarity-B" edges. Edges 59, 60, and 61 were straight edges and were not assigned polarity. The images were enclosed within a thin-line rectangle.

As can be seen in Figure 1, there were three fiducial marks located outside each corner of the rectangle. The lines forming each mark were parallel to two sides of the rectangle and were 600 microns long. The widths of the lines of the three fiducial marks at each corner were different. The lines forming the outside marks were 10 microns wide, those of the intermediate marks were 7 microns wide, and the lines of the marks closest to any corner of the rectangle were 5 microns wide. The operators preferred the mark formed by the lines 10 microns wide because it was best suited to the measuring instrument. Consequently this was the mark used as a reference coordinate for all measurements.

10

MASTER PLATE

The array of shapes portrayed in Figure 1 was produced in a large format. The geometric shapes were scribed in a Rubylith scribing material, using precision instruments. A greatly reduced copy of the format was then produced on a very high-resolution, high-contrast photographic plate. This plate is hereafter referred to as the "master plate."

GEMS

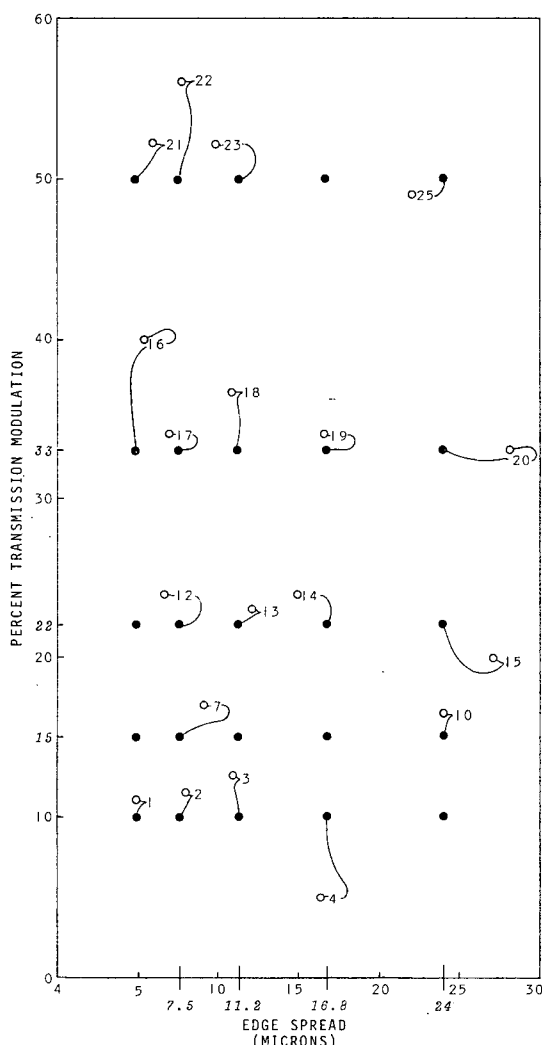


Figure 2. Planned (closed points) and obtained (opened points) modulation and edge spread values for each Gem.

The master plate was used to produce 19 photographic transparencies, Gems. The Gems were made⁴ by reproducing the master plate on Kodak High-Definition Aerial Film, Type 3404, which was then contact-printed onto Kodak Fine-Grain Aerial Duplicating Film, Type 8430. These two types of film were selected because they are used in many operational reconnaissance programs. A mean image density of 1.0 for both films was selected since 1.0 is representative of the mean density of aerial photographs produced in many operational programs. The reproduction of the master plate onto Type 3404 film was such that its contact print made on Type 8430 exhibited the desired image modulation and edge spread.

The closed points plotted in Figure 2 depict the modulation and edge spread planned for each of the Gems and the open points in the figure depict the obtained modulation and edge spread characteristics. The deviation of the obtained values from those planned was considered sufficiently small to warrant accepting the Gems for use in the experiment.

⁴ For a detailed description of the procedure see Appendix B.

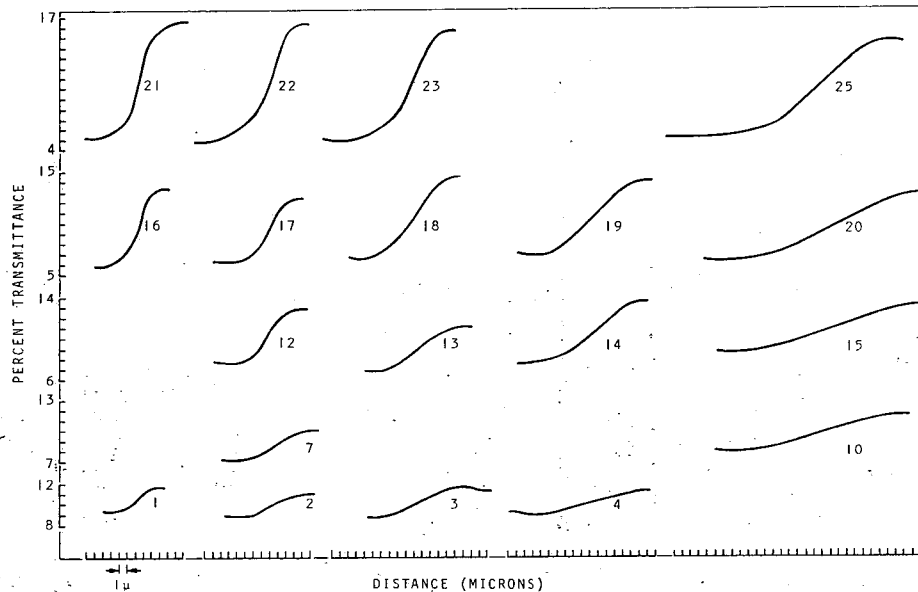


Figure 3. Edge gradients of the Gems.

Figure 3 shows plots of the edge gradients for each of the Gems produced. Because of the granular structure of the film, a single microdensitometer trace is not a very reliable description of the true edge gradient. Therefore the average of three microdensitometer traces was obtained by superimposing the three traces. Figure 3 shows the average microdensitometer traces. Figure 4 illustrates an example of the superimposition of three traces and the method used to measure and describe the edge spread and modulation.

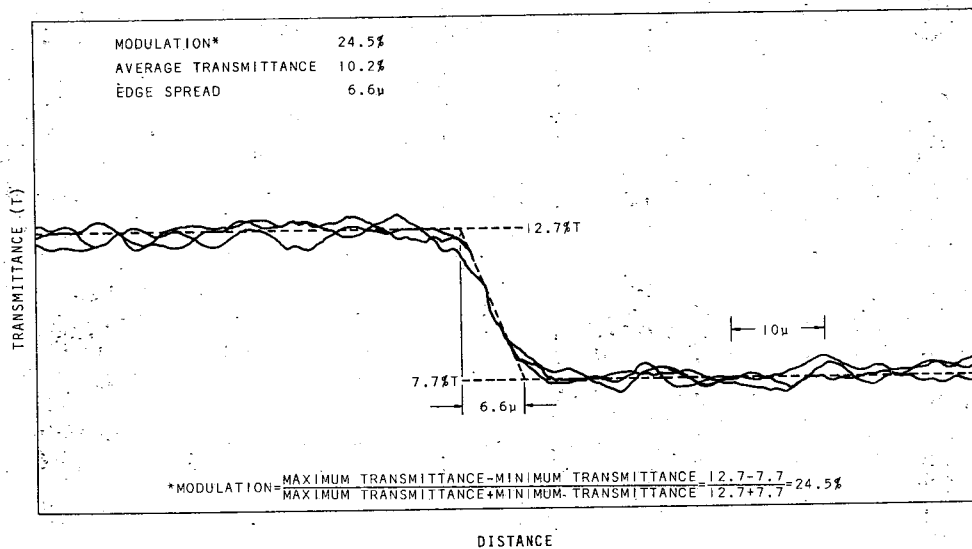


Figure 4. Superimposition of three microdensitometer traces and the method used to measure and describe the edge spread and the modulation.

The edge gradient of the optical image incident on the Type 3404 film corresponded to a Gaussian-shaped modulation transfer function, i.e., the images used in the experiment simulated the characteristics of an aerial camera forming optical images with Gaussian-shaped point-spread functions. But, the edge gradients of the images on the Type 3404 film were not necessarily Gaussian because of the nonlinear response of the film.

The Gems were mounted between two small pieces of microscope cover glass for protection and for convenience in inserting and removing them from the measuring equipment.

SUBJECTS AND EQUIPMENT

The subjects were six operators experienced at measuring photographic images. Their experience ranged from three-quarters of a year to nine years with a mean of four years.

The operators used a Mann 621 Comparator for all measurements. The Mann 621 Comparator, shown in Figure 5, is a binocular viewing device that has controls for varying the intensity of transillumination, magnification, focus, and for

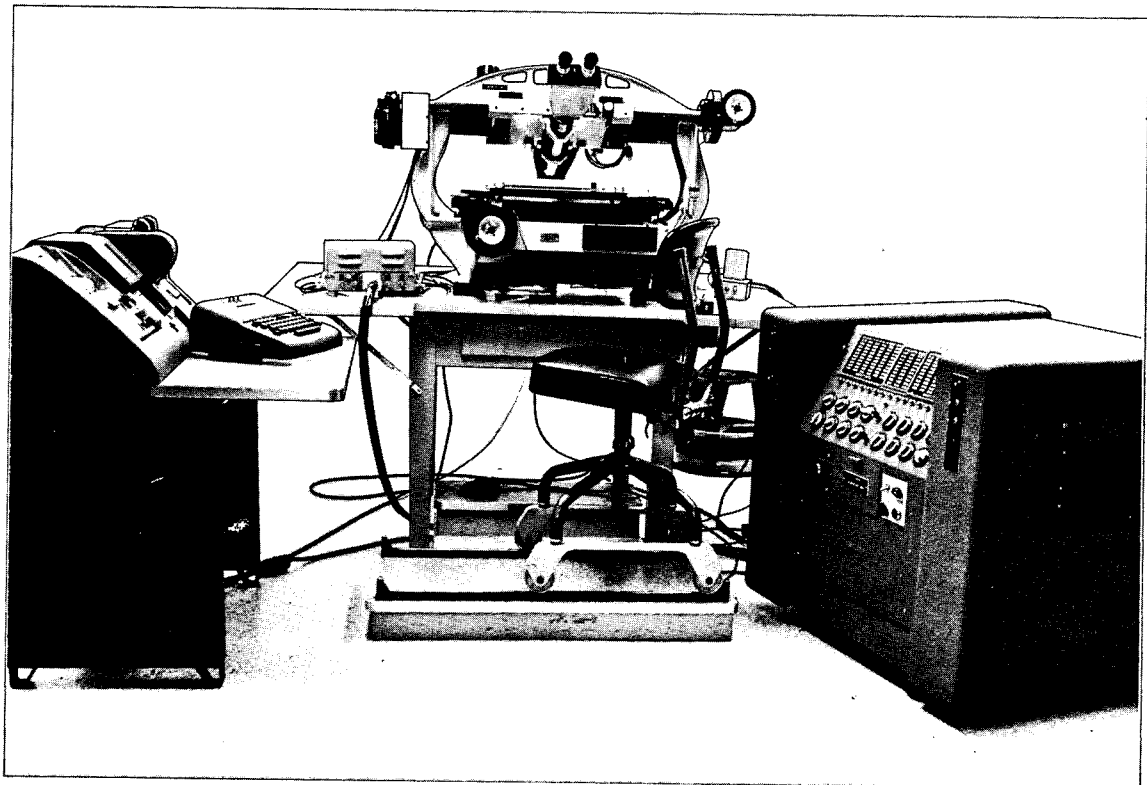


Figure 5. Mann 621 Comparator, center. Data translator (right) and IBM card puncher (left).

rotating the stage on which the photograph is placed. An X and a Y control knob are used to place a cross-hair (located in the ocular) on an edge. The device was calibrated just prior to the experiment.

An IBM card punch was linked to the Mann 621 via a data translator. When the operator had satisfactorily positioned the edge he pressed a foot pedal and the X and Y coordinates of the position were automatically recorded on a card.

EXPERIMENTAL DESIGN AND PROCEDURE

The operator's task was to position each of the four fiducials and the 57 edges on the master plate and on each Gem to be coincident with the ocular reticle. He first measured the fiducial marks and edges on the master plate and then measured each of the 19 Gems. The order of administration of the Gems, with respect to the identifying numbers in Table 1, was 13, 3, 7, 22, 18, 4, 15, 20, 17, 10, 25, 12, 14, 2, 19, 23, 21, 16, and 1. There was about a one week interval between the administration of each Gem to any one operator.

The operators rotationally aligned the stage so that the vertical reticle line was parallel with the line labeled "start" in Figure 1. The fiducials were always positioned first and in the same order, viz., lower left, upper left, upper right, lower right. The order in which an operator positioned the edges of the Gems was varied randomly from one Gem to the next, and the order was different for each operator. These orders of positioning were given to each operator in the form of a numbered list and a large copy of Figure 1, with numbered edges.

INSTRUCTIONS

Before each operator began the first experimental session he was read the following instructions:

The purpose of this experiment is to investigate mensuration accuracy as a function of image resolution, contrast, image size and shape. We are not interested in measuring your individual performance. However, we are interested in having you make measurements as accurately as you can. Please use the same measurement techniques in the experiment as you use in your daily work.

After you have placed the appropriate photograph on the stage, spend about ten minutes looking at it to stabilize your vision. Then select the

magnification you wish to use and adjust the focus control. Do this by looking at some of the edges and not at the fiducial marks at the corners of the photograph. Once you have selected a magnification level and adjusted the focus, do not change them during the session. However, you may adjust the intensity of the light source whenever you wish.

Note the images are not symmetrical and consequently there are no common X-Y points on the edges to be positioned. In other words you must change the X-Y position of the cross-hair when going from one edge to the next. Use the dot at the intersection of the cross-hair to position each edge.

Although we are primarily interested in the accuracy of mensuration in the X dimension, we also want you to measure as accurately as you can in the Y dimension. To measure in the Y dimension follow these rules. For the straight edges on the right side of the photograph place the center of the cross-hair on edge 37. Then move the cross-hair in the X dimension toward the edge you wish to measure. For edges 59, 60, and 61 bisect the Y dimension of the edge, for radii place the cross-hair tangent to the arc and for angles place it at the vertex of the angle.

Position each edge three times. After you have positioned each set of ten edges, go back to the fiducial number 1 (lower left hand corner of the photograph) and check the readout you get. The purpose of the check is to determine whether the equipment is drifting. If the equipment is drifting, please notify the experimenter. Work at your own speed and rest whenever you wish. Now are there any questions?

The following information was automatically punched on a card after each positioning: (1) operator number, (2) Gem number, (3) magnification, (4) order number of the edge, (5) edge number, (6) positioning number for each edge (1, 2, or 3), (7) X position in microns, and (8) Y position in microns.

COMPUTATION OF POSITIONING ERRORS

Measurements of the master plate provided data used to spatially relate the edges to the fiducial marks and thus provide the true position of the edges relative to the fiducial marks. Image distortions due to physical changes in film occur during the fabrication, storage, and use of the Gems. Consequently the spatial relations among each of the four fiducial marks on each Gem may be different from those on the master plate. Accordingly, the measurement of the fiducial marks of each Gem provided information on the direction and magnitude of the distortions. After analytically accounting for such distortions, the true positions of the edges in each Gem are known. The discrepancy between the true edge position and the position indicated by the operator was the positioning error.

The correction of the image distortions in the Gems was performed as follows: A mean of the measurements made by the six operators was calculated for each edge and each fiducial on the master plate. In addition, a mean of the measurements made by each operator was calculated for each fiducial on each Gem. Least squares theory was applied to form normal equations from those means. The solution of the equations produced coefficients for rotation, translation, scale change in the X and Y directions, and orthogonalization of the coordinate system. These coefficients were then applied to establish the positions of the edges of each Gem. For each operator three X and Y positioning errors were computed for each edge on each Gem. The positioning errors were the difference between the value obtained for an edge on the master plate and for the corresponding edge on the Gems.

The positioning errors were inspected and two percent of them were discarded because they were suspected to be a result of improper operation of the instrument or positioning of edges in the wrong order. A positioning error was discarded if it was in excess of about 50 microns in the X or Y dimension.

A mean of the three X position errors was computed for each operator for each of the 57 edges on each of the 19 Gems. The results described in this report are based on those means and are hereafter referred to as "pointing errors." The Y position errors were not analyzed because the edges were oriented so that only X position errors were meaningful.

Chapter IV

ANALYSES AND RESULTS

THE PRECISION OF POINTING ON THE MASTER PLATE

The edges on the master plate were very sharp high-contrast images. These edges, which can be considered as "ideal" edges, were of far better quality than those encountered in aerial photographs. The first analyses of the data were made to determine the magnitude of the differences among operators (standard deviations) in positioning these "ideal" edges.

A standard deviation⁵ of the X-coordinate values was computed for each edge and for fiducials 2, 3, and 4 on the master plate. (A standard deviation could not be computed for fiducial number 1 because all operators set the X coordinate at zero for this fiducial.)

Inspection showed no relation between the magnitude of the standard deviations and,

- (1) the size of straight edges and of curved edges
- (2) the length of the radius.

However, there was a relation between the magnitude of the standard deviations, and

- (1) the size of pointed edges (angles)
- (2) the acuteness of the angle
- (3) edge polarity.

In those instances where there was no relation between the magnitude of the standard deviation and a variable, the standard deviations were averaged by taking the square root of the mean of the variances.

⁵ The standard deviation is an index of variability. In a normal (Gaussian) distribution, the standard deviation is interpreted as the values between which about two-thirds of the observations lie. For example, if the standard deviation is 2, two-thirds of the observations lie between ± 2 units of the mean value.

TABLE 4

AVERAGE STANDARD DEVIATIONS (IN MICRONS)
OF THE X-COORDINATE VALUES FOR THE FIDUCIALS,
STRAIGHT AND CURVED EDGES ON THE MASTER PLATE

	FIDUCIALS	STRAIGHT EDGES (RECTANGLES)	POLARITY A CURVED EDGES (RADI)	POLARITY B CURVED EDGES (RADI)
AVERAGE STANDARD DEVIATION	1.0	2.1	1.4	2.1
RANGE OF STANDARD DEVIATIONS	0.6-1.1	1.1-3.2	0.9-2.0	1.5-2.9
NUMBER OF STANDARD DEVIATIONS	3	3	9	9

TABLE 5

STANDARD DEVIATIONS (IN MICRONS)
OF THE X-COORDINATE VALUES FOR THE
POINTED EDGES ON THE MASTER PLATE

		POLARITY A POINTED EDGES (ANGLE IN DEGREES)				POLARITY B POINTED EDGES (ANGLE IN DEGREES)			
		22	45	90	135	22	45	90	135
EDGE SIZE (IN MICRONS)	48	4.1	1.5	1.7	0.8	3.9	2.4	1.9	1.8
	96	3.1	2.1	2.0	1.6	3.7	2.5	2.1	2.1
	190	2.6	3.7	2.4	2.5	2.5	3.1	2.9	2.6

Inspection of Tables 4 and 5 shows that the standard deviations for the polarity-B edges were slightly larger than those for polarity-A edges, but the differences were small, being of the order of 0.5 micron. In addition it can be seen from Table 5 that the standard deviation increased as the angle became more acute, and, with the exception of the angles of 22 degrees, it increased as the size of the edge increased.

In summary, some two-thirds of the operators positioned "ideal" edges within the range of ± 1 to about ± 4 microns of the true location. In addition, the magnitude of the standard deviation was shown to depend on the edge shape, the acuteness of the angle, the edge polarity, and on the size of the pointed edges (angles).

PRELIMINARY ANALYSES OF THE POINTING ERRORS FOR EDGES ON THE GEMS

Preliminary statistical tests were performed of both the means and the standard deviations of the pointing errors on the Gems. These tests were performed separately for each Gem (edge spread-modulation combination) to determine whether or not the angularity, the curvature, or the size of the edge affected either the mean or standard deviation of the pointing errors. The tests, in conjunction with inspection of the results, were used primarily to assess which variables could be disregarded in the final description of the means of the pointing errors.

Means of the Pointing Errors

Five analyses of variance of the mean pointing errors were performed for each of the 19 Gems, resulting in a total of 95 analyses. The five analyses were as follows: pointed edges (4 angles) by edge size, one for polarity-A and one for polarity-B; curved edges (4 radii) by edge size, one for polarity-A and one for polarity-B; and one for the size of straight edges (rectangles).

A summary of the analyses and the conclusions follow:

1. The differences among the mean pointing errors for the three edge sizes were statistically significant ($p < .05$) in 33 of the 95 analyses, but the differences among means were usually about two microns or less. Inspection showed that from one Gem to the next the mean error for any one edge size was not consistently larger or smaller than that for another edge size.

Because the differences among means were small and inconsistent it was concluded that the edge size did not affect the mean of the pointing errors for any of the edge shapes.

2. The differences among the mean pointing errors for the four radii were statistically significant ($p < .05$) in 14 of the 38 analyses (2 polarities x 19 Gems), but again the differences among means were about two microns or less. Inspection showed that from one Gem to the next the mean error for any one radius was not consistently larger or smaller than that for other radii.

Because the differences among means were small and inconsistent, it was concluded that the amount of curvature (radius) of the edge did not affect the mean of the pointing errors.

3. The differences among the means of the pointing errors for the four angles were statistically significant ($p < .05$) in 25 of the 38 analyses (2 polarities x 19 Gems). In the 25 analyses where there were significant differences among means, the mean error increased as the angle decreased. The same relation was observed in 9 of the 13 analyses in which the differences were not statistically significant.

It was concluded that the acuteness of the angle affected the mean of the pointing errors.

4. In addition to the results reported above, inspection showed no consistent differences between the mean error for straight edges and polarity-B curved edges from one Gem to the next.

It was concluded that there was no difference in the means of the errors for polarity-B curved edges and for straight edges.

Standard Deviations of the Pointing Errors

Five statistical analyses of the standard deviations were performed for each of the 19 Gems. These analyses were performed for the same combination of variables described in the previous section.

A summary of the analyses and the conclusions follow:

1. The differences among standard deviations were statistically significant ($p < .05$) in only 6 of the 38 analyses of curved edges (radii) by edge size. In addition, in each of these 6 analyses no more than two of the standard deviations were statistically different from the remainder, and there was no systematic change in the standard deviations as a function of the radius length or edge size.

It was concluded that the amount of curvature and the size of curved edges did not affect the standard deviations of the pointing errors.

2. The differences among standard deviations were not statistically significant in any of the 19 analyses of the size of straight edges.

It was concluded that the size of straight edges did not affect the standard deviations of the location errors.

3. The differences among standard deviations were statistically significant in 19 of the 38 analyses of pointed edges (angles) by size. The statistical significance was usually due to the acuteness of the angle. The results showed that in 33 of the 38 analyses the magnitude of the standard deviations increased as the angle decreased. However, there was no systematic change in the standard deviations with changes in edge size.

Thus, there was no apparent relation between the magnitude of the standard deviations and the edge sizes, but there was a relation between the magnitude of the standard deviations and the acuteness of the angles.

4. Inspection showed no systematic differences in the standard deviations for polarity-B curved edges and straight edges.

Combination of Variables Within Gems

As a result of the preliminary analyses, it was concluded that edge size for all edge shapes, amount of edge curvature, and polarity-B curved edges versus straight edges did not affect pointing errors. Consequently these data were pooled and 10 new error scores were computed for each operator for each of the 19 Gems. These scores were as follows:

1. A mean pointing error for each of the four polarity-A angles and each of four polarity-B angles. Each score was the mean of the pointing errors for the three edge sizes.
2. A mean pointing error for what will be referred to hereafter as polarity-B curved/straight edges. This score was the mean of the pointing errors for the nine polarity-B curved edges (radii by size, polarity-B) and those for the three straight edges.
3. A mean pointing error for polarity-A curved edges. This score was the mean of the pointing errors for the nine polarity-A curved edges.

An average standard deviation was computed for each of the ten sets of edges for each Gem. The standard deviation for each of the eight pointed edges (angles) was the average of the standard deviations for the three edge sizes. The standard deviation for the polarity-B curved/straight edges was the average of the standard deviations for the nine curved edges and the three straight edges, and for the polarity-A curved edges it was the average of the standard deviations for the nine curved edges.

THE EFFECTS OF THE EDGE SPREAD, MODULATION, SHAPE,
AND POLARITY OF THE EDGE ON THE MEANS
AND THE STANDARD DEVIATIONS OF THE POINTING ERRORS

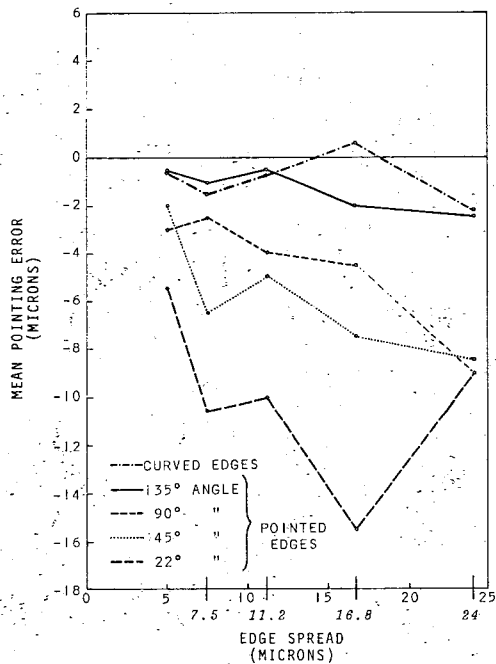


Figure 6. Mean pointing error for polarity-A edges as a function of edge spread. All modulations combined.

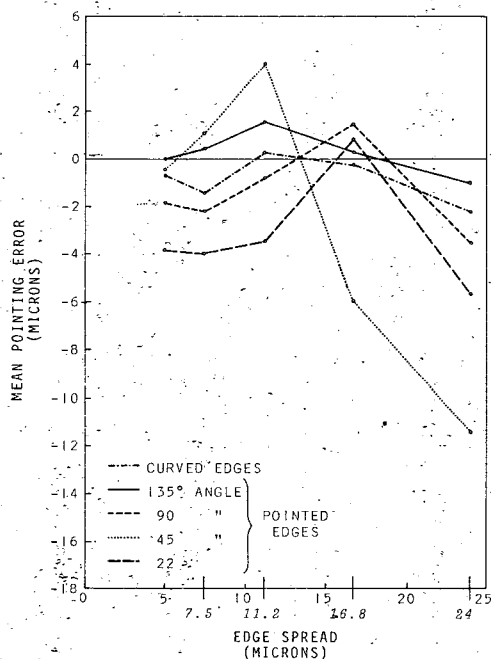


Figure 7. Mean pointing error for polarity-B edges as a function of edge spread. All modulations combined.

Means of the Pointing Errors

The mean error for each edge was plotted as a function of modulation and edge spread. The magnitude of the mean pointing error was not systematically related to the modulation. Inspection of the results showed a slight tendency for the mean error to increase as the modulation decreased, but this tendency was not consistent across edge spreads or from one edge shape to another.

To increase the reliability of the means, a mean pointing error was computed for each edge at each edge spread by averaging across modulations. In other words, modulation was disregarded as a variable in the description of the mean errors.

Figures 6 and 7 show the mean pointing errors for edges of both polarities as a function of edge spread. Negative values indicate the mean location was to the left of the true edge, and positive values indicate that it was to the right of the true edge. (See Figure 1 for the orientation of the edges). A negative error for polarity-A edges indicates the mean pointing was on the more transparent side of the edge and a positive error indicates it was on the more opaque side of the edge; the converse was true for polarity-B edges.

The results for polarity-A edges show that there was a general negative error for all edges and little or no difference in the error for curved edges and the

angles of 135 degrees. In addition, the negative error increased as the edge spread increased and the angle decreased. The results for polarity-B edges, unlike those for polarity-A edges, were not consistent. There was a slight general negative error and possibly a slight increase in the negative error as the angle decreased.

Two peculiarities of the results were apparent for polarity-B edges (Figure 7). First, the curve for the angle of 45 degrees was not consistent with those for the remaining edges. The results indicated that there was something unusual about this edge, but visual inspection of the edges on both the master plate and the Gems revealed no artifact. Nevertheless, the data appeared suspect so the mean errors for edges of 45 degrees, polarity-B, were disregarded.

Second, the mean error for all edges combined was slightly negative at the smallest edge spread, decreased to about zero at edge spreads between 11 and 16 microns and again was slightly negative for an edge spread of about 24 microns. As this same relation held for each edge the general relation appeared to be reliable. (Whether or not the relation was in fact reliable is of little practical significance because the change in the mean error was quite small for each edge shape.)

A comparison of the results in Figures 6 and 7 shows that for pointed edges of 90 degrees or less, the mean errors are much larger for the polarity-A edges than for the polarity-B edges, particularly at the larger values of edge spread and for the most acute angle.

Standard Deviations of Pointing Errors

As stated earlier, there was no apparent relation between the mean pointing error and modulation so the means of the pointing errors were averaged across modulations. There was, however, a relation between the standard deviation and modulation; consequently the standard deviations were not averaged across modulation.

The magnitudes of the standard deviations as a function of modulation and edge spread are plotted for polarity-A edges in Figures 8 through 12 and for polarity-B edges in Figures 13 through 17. Each figure shows the results for one type of edge.

Each figure shows the same general relation between the standard deviation, modulation, and edge spread. Although the relation is not perfectly systematic for each edge, the data indicate little or no systematic difference between the standard deviations for the three highest values of modulation

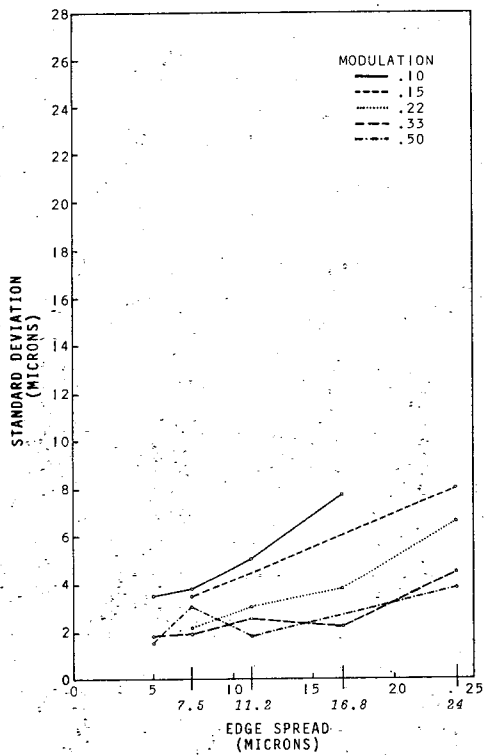


Figure 8. Standard deviations of the pointing errors for polarity-A curved edges as a function of modulation and edge spread.

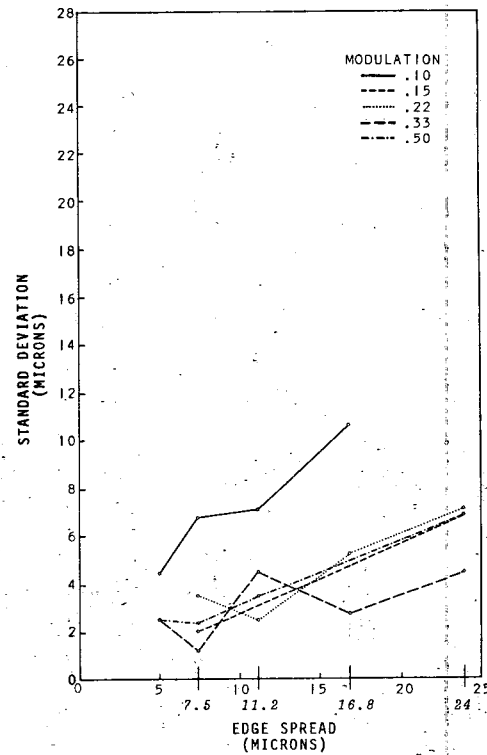


Figure 9. Standard deviations of the pointing errors for polarity-A 135° angles as a function of modulation and edge spread.

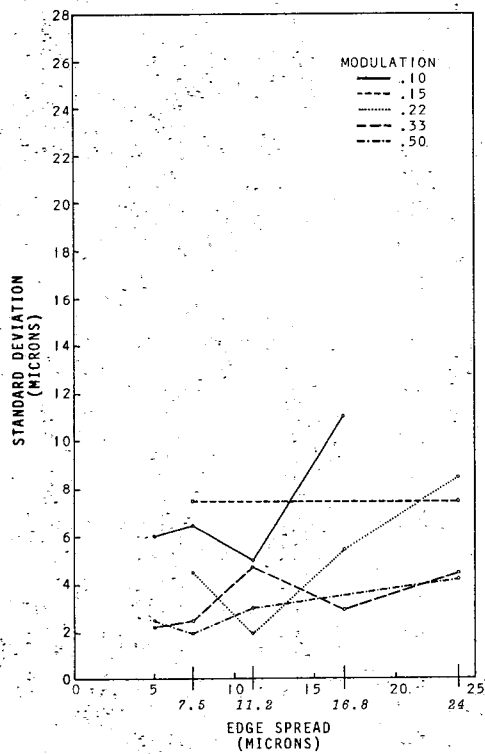


Figure 10. Standard deviations of the pointing errors for polarity-A 90° angles as a function of modulation and edge spread.

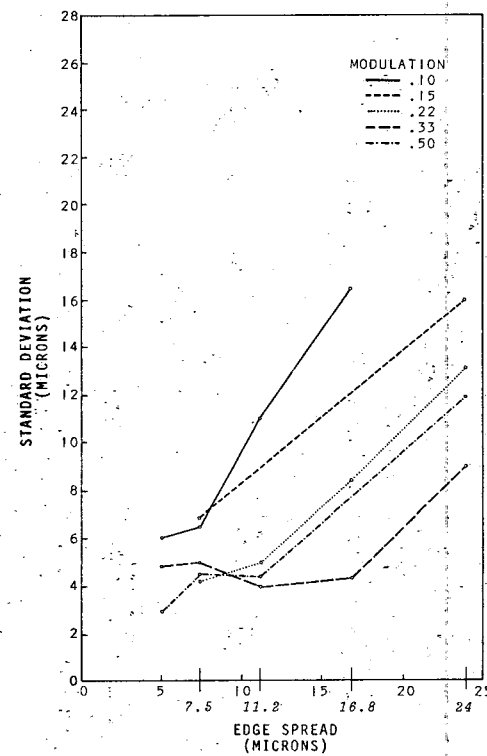


Figure 11. Standard deviations of the pointing errors for polarity-A 45° angles as a function of modulation and edge spread.

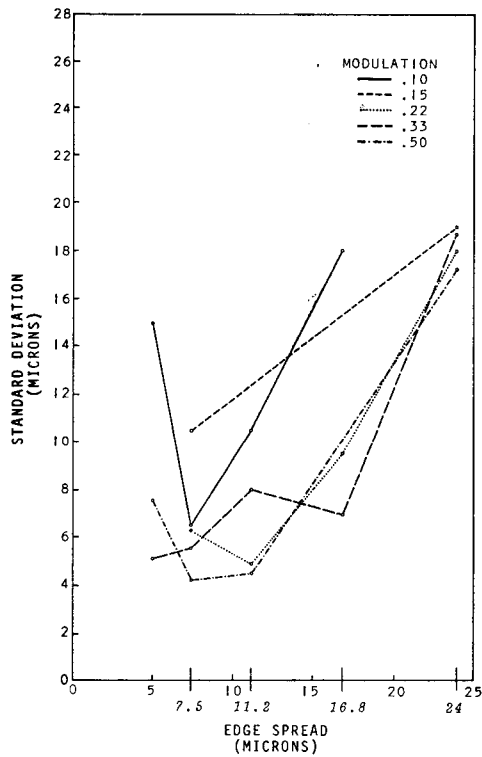


Figure 12. Standard deviations of the pointing errors for polarity-A 22° angles as a function of modulation and edge spread.

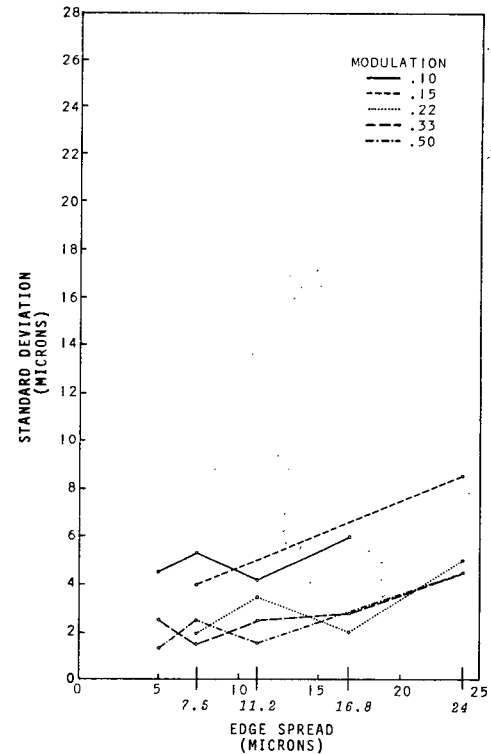


Figure 13. Standard deviations of the pointing errors for polarity-B curved/straight edges as a function of modulation and edge spread.

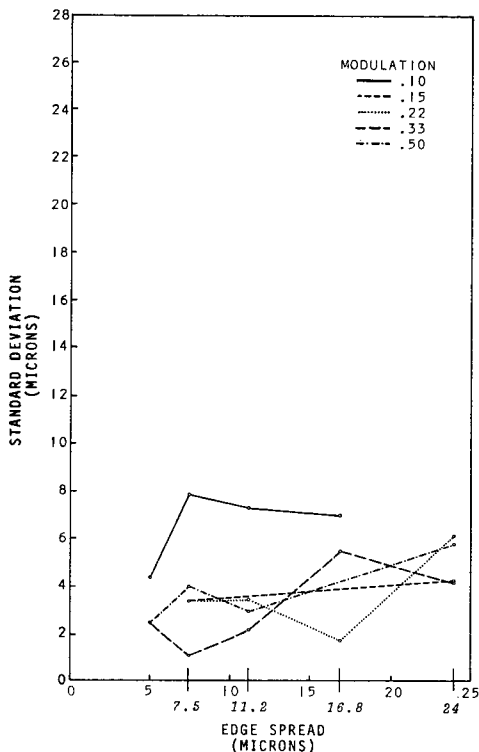


Figure 14. Standard deviations of the pointing errors for polarity-B 135° angles as a function of modulation and edge spread.

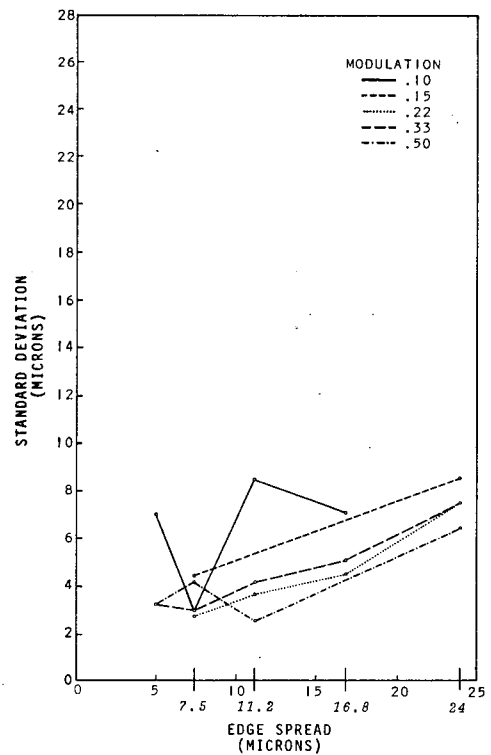


Figure 15. Standard deviations of the pointing errors for polarity-B 90° angles as a function of modulation and edge spread.

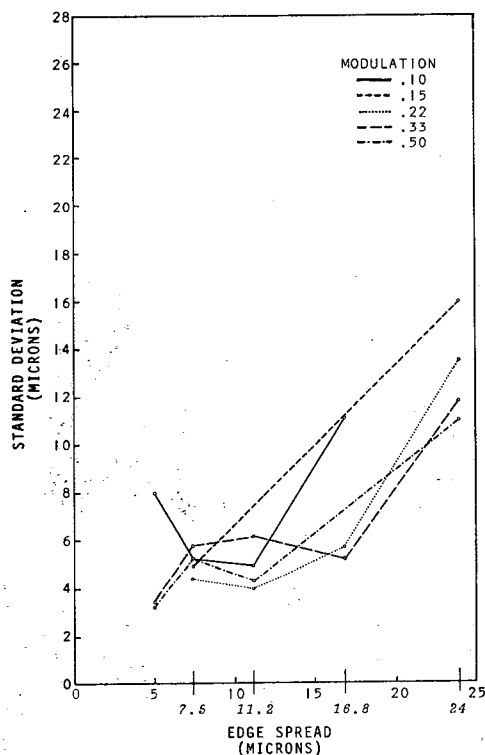


Figure 16. Standard deviations of the pointing errors for polarity-B 45° angles as a function of modulation and edge spread.

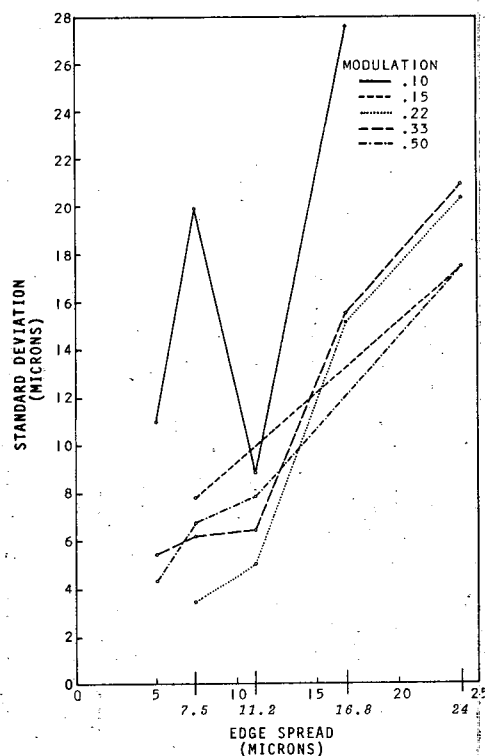


Figure 17. Standard deviations of the pointing errors for polarity-B 22° angles as a function of modulation and edge spread.

(.22, .33, and .50), a slightly larger standard deviation for a modulation of .15 than for the three higher modulations, and a larger standard deviation for a modulation of .10 than for the four largest modulations. In addition, the results showed that the magnitude of the standard deviation: (1) increased as the edge spread increased and this increase was larger for the more acute angles, and (2) increased as the acuteness of the angle increased.

If the curves for a modulation value of .10 are disregarded (the images of these edges were barely visible), it is apparent that the magnitude of the standard deviation was affected more by edge spread than by modulation.

Operator Errors in Measuring the Extent of Images

The accuracy (mean) and precision (standard deviation) of the operators' measurements of image extent--or the distance between edges--can of course be calculated from the mean and the standard deviations of the pointing errors. On the other hand, a very large variety of image shapes may be generated from combinations of the edge shapes included in this experiment and the cost of making the required calculation for every possible image shape for each combination of edge spread and

modulation would be prohibitive. Instead, the data and rules required for computing the mean and standard deviation of image extents are given in Appendix A.

THE MEASUREMENT OF BAR WIDTHS

Preliminary statistical tests were performed on both the means and standard deviations of the operators' errors in measuring widths of bars. These tests in conjunction with visual inspection of the data were used to assess which experimental variations could be disregarded in the final description of the results.

Preliminary Analyses--Mean of Measurement Errors

A measurement error was computed for each operator for each of the six bars on each of the 19 Gems. The measurement error for each bar was obtained by subtracting the pointing error of the left edge from that of the right edge. Each of the six operators had six measurement errors, one for each bar, on each of the 19 Gems.

An analysis of variance of the measurement errors was computed for each Gem (modulation-edge spread combination) to test the effects of the width and the transmittance of the bars on the mean measurement error. The results of the 19 analyses showed that the differences between the mean error for the low transmittance and high transmittance bars were statistically significant ($p < .05$) in ten of the 19 analyses. In each of those ten analyses, the mean error was larger for the low transmittance bars. In addition, the mean error was larger for the low transmittance bar than it was for the high transmittance bars in seven of the nine analyses in which the differences between means were not statistically significant. The analyses also showed that the differences among the mean errors for the three widths (6, 12, and 24 microns) were statistically significant ($p < .05$) for 12 of the 19 Gems, and for all 19 Gems the mean error increased as the width decreased. It was concluded that the width and the polarity of the bars affected the mean measurement error.

To determine whether modulation and edge spread affected the mean measurement error, the mean error for each of the six bars was plotted as a function of modulation and edge spread. Inspection showed no consistent relation between the mean error and level of modulation from one width to another. Consequently, modulation was disregarded as a variable in presenting the mean measurement errors. The results did show a consistent relation between the mean error and edge spread--the mean error increased as the edge spread increased.

Preliminary Analyses--Standard Deviations of Measurement Errors

25X1

Six standard deviations of the measurement errors were computed--one for each of the six bars in each Gem. A statistical analysis () of the significance of differences among the six standard deviations was made for each of the 19 Gems. The results of the analyses showed that the differences among standard deviations were statistically significant ($p < .05$) in only three of the 19 analyses, and in each of those three analyses, only one standard deviation was statistically different from the others. It was concluded that neither the bar width nor the polarity of the bar affected the magnitude of the standard deviations.

To determine whether modulation and edge spread affected the standard deviations, the standard deviations for each bar were plotted as a function of modulation and edge spread. Inspection showed no consistent differences among the standard deviations for the four higher modulations (.15, .22, .33, and .50). The only consistent difference was between the lowest modulation (.10) and the four highest modulations. In addition, there was an increase in the magnitude of the standard deviations for edge spread values in excess of about 11 microns.

In light of the results described above, an average standard deviation was computed at each edge spread for bars of .10 modulation, and for bars of .15 to .50 modulation combined. The average standard deviations for bars of .10 modulation was the average of six standard deviations (2 polarities x 3 bar widths), and that for bars of .15 to .50 modulation was the average of 24 standard deviations (2 polarities x 3 line widths x 4 modulations).

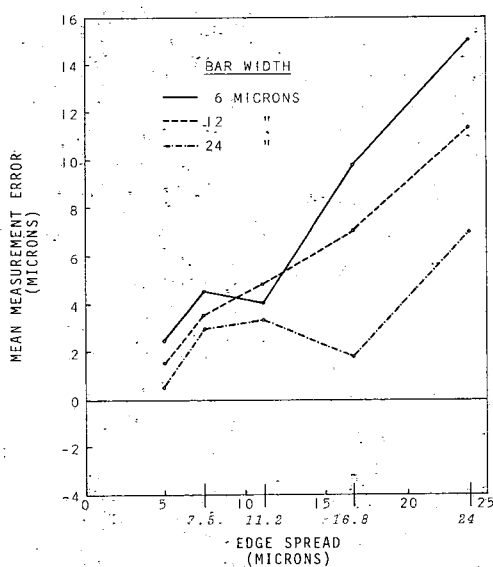


Figure 18. Mean measurement error for low transmittance bars as a function of edge spread and bar width. All modulations combined.

Means and Standard Deviations of Measurement Errors

Figures 18 and 19 show the means of the measurement errors as a function of edge spread and the bar widths. The positive values on the ordinate indicate the magnitude of overestimation of bar widths and the negative values indicate underestimation of the bar widths. For example, in Figure 18 the 12-microns-wide bar that had an edge spread of 11.2 microns was overestimated by about 5 microns; that is, it was measured as 17 microns wide.

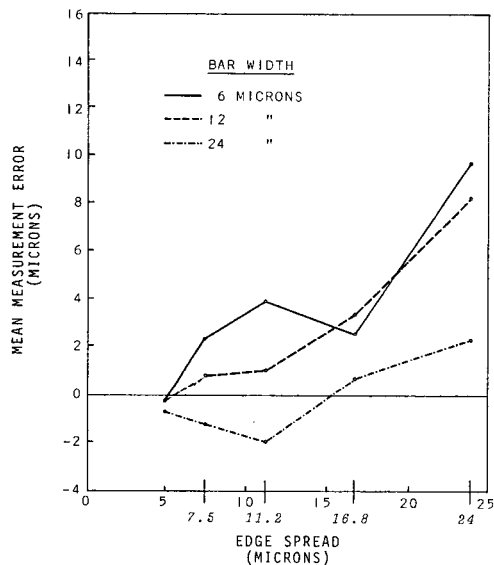


Figure 19. Mean measurement error for high transmittance bars as a function of edge spread and bar width. All modulations combined.

Figures 18 and 19 show the same general relation between the width of the bar, edge spread, and the mean measurement error. With the exception of the high-transmittance, 24-micron-wide bar, overestimation of the width increased as the edge spread increased. This increase in overestimation was greatest for bar widths of 6 microns and 12 microns and least for a bar width of 24 microns.

A comparison of the results in Figures 18 and 19 shows an obvious difference in the measurement errors of low and high transmittance bars. The widths of the low transmittance bars were overestimated more than were the widths of the high transmittance bars. This was true for each of the bar widths and at all edge spreads.

TABLE 6
AVERAGE STANDARD DEVIATIONS IN MICRONS OF MEASUREMENT ERRORS FOR THE FIVE EDGE SPREADS AND FOR .10 MODULATION AND FOR .15 TO .50 MODULATIONS COMBINED

MODULATION	EDGE SPREAD (MICRONS)				
	5.0	7.5	11.2	16.8	24.0
.15 TO .50	2.2	2.0	2.1	3.0	7.5
.10	2.7	3.6	3.5	7.5	—*

*THE GEM REPRESENTING THIS CELL WAS NOT INCLUDED IN THE EXPERIMENT.

Table 6 shows the average standard deviations of the measurement errors for the five edge spreads and for .10 modulation and for .15 to .50 modulations combined. The results show that for all modulations the standard deviations remained constant up to an edge spread of 11.2 microns and then increased.

Chapter V

DISCUSSION AND APPLICATION OF RESULTS

QUALIFICATION OF THE RESULTS

The purpose of the present experiment was to provide estimates of the accuracy and precision with which operators measure different kinds of photographic images. Although the purpose was achieved, the reliability of some of the estimates was lower than desired. This low reliability was, in part, a result of using too few (six) operators.

There are two consequences of low reliability. First, some of the estimates provided may differ considerably from the true (population) means and standard deviations. Second, there is a lower likelihood of detecting real differences in measurement errors as a function of an experimental variable. For example, in this experiment it was concluded that the level of modulation did not affect the mean measurement error. Although the results seemed to warrant this conclusion, it may be that the low reliability precluded the detection of real differences among the means.

The implications of the above discussion are that (1) the means and standard deviations described in this report are statistics and, as such, should be interpreted as approximations of the true (population) values, and (2) a much larger number of operators, at least 25 or 30, should be used in studies of measurement errors.

ATTEMPTS TO RELATE ACTUAL EDGE POSITIONS WITH POINTING ERRORS

Since it would be desirable to predict the accuracy of pointing from the position of the actual edge on the density gradient of the edges, the following examination was made: The positions of the actual edge on the optical density edge-gradients of several Gems was determined using microdensitometry. The position of the edge on the gradient differed among Gems. Attempts were made to relate the mean pointing errors to the positions of the actual edge, but the instability of the means of the pointing errors was such that no relation was apparent.

THE RELATIVE CONTRIBUTIONS OF EDGE SPREAD AND MODULATION TO MEASUREMENT

The results indicated that differences in edge spread contribute more to both the precision and accuracy of measurement than do differences in modulation. A change in the edge spread from 5 to 24 microns increased the standard deviation of the pointing errors by about 3 microns for curved and straight edges, and by about 14 microns for an angle of 22 degrees. The mean pointing error also increased by about 5 or 6 microns for the more acute angles. In addition, the mean error in measuring bar widths increased by a few microns for a 24-micron wide bar and by as much as 10 or 12 microns for a 6-micron wide bar.

Changes in the modulation had no effect on the mean error. In addition, changes in modulation from .50 to .22 had little or no effect on the standard deviations. The standard deviations increased only when the modulation was reduced to about .15 or .10--a modulation so low that the image was barely visible.

It would seem reasonable to conclude that increases in modulation beyond .22 would not improve the accuracy or precision of the operators' measurements. But, a reduction of the edge spread would result in a substantial improvement in both the accuracy and the precision of measurement.

APPLICATION OF RESULTS

The results described in Appendix A should be used to predict the measurement error for images formed by edges that do not have overlapping edge spreads; that is, the distance between the edges should be greater than the edge spread. This position is supported by the results for bars which showed that the mean measurement error increased when there was an overlap in the edge spread of the edges forming the bar.

One obvious application of the results is to avoid, if possible, the estimation of image length (or distances) from the location of pointed edges, particularly when the edge is a 90 degree angle or less and has a polarity of A. The results showed that, in general, the location of pointed edges was less accurate and less precise (less agreement among operators) than the location of straight or curved edges.

APPENDIX A











THE COMPUTATION OF THE MEAN AND THE
STANDARD DEVIATION OF MEASUREMENT ERRORS

In this section the rules will be given for computing the mean and the standard deviation of the operators' measurements of images (or distances between edges). Several examples of different image shapes will be given to illustrate and clarify the rules.

The Mean of Measurement Errors

Table 1A shows the mean of the pointing errors at each edge spread for the different edge shapes and the two polarities. A negative mean indicates the mean error was to the left and a positive mean indicates it was to the right of the edges shown in the table.

TABLE 1A
MEAN POINTING ERROR (IN MICRONS) FOR THE DIFFERENT
EDGE SHAPES AND THE TWO POLARITIES
AT EACH EDGE SPREAD. ALL MODULATIONS COMBINED.

		EDGE SPREAD (MICRONS)				
		5.0	7.5	11.2	16.8	24.0
POLARITY-A EDGES	 CURVED EDGES	-0.6	-1.6	-0.9	0.7	-2.3
	 135°	-0.4	-1.1	-0.7	-2.1	-2.6
	 90°	-3.0	-2.3	-3.9	-4.3	-9.1
	 45°	-1.9	-6.6	-4.8	-7.6	-8.4
	 22°	-5.4	-10.2	-9.9	-15.4	-9.0
POLARITY-B EDGES	 CURVED/ STRAIGHT EDGES	-0.8	-1.5	+0.3	-0.3	-2.3
	 135°	0.0	+0.4	+1.5	+0.3	-1.1
	 90°	-1.9	-2.2	-0.8	+1.4	-3.6
	 45°	-2.9	-3.1	-2.2	-1.1	-4.7
	 22°	-3.9	-4.0	-3.5	+0.8	-5.8

*THE VALUES REPORTED FOR THIS EDGE ARE THE MEANS OF THE
90° AND 22° EDGES AT EACH EDGE SPREAD (SEE PAGE 23 OF THE
REPORT FOR AN EXPLANATION).

To compute the mean measurement error for a given image, one must determine whether the mean for each of the two edges is inside or outside the image. Of course, the position of the mean depends on the orientation of the edges forming the image. So, the mean measurement error for an image is computed by either adding, adding and changing the sign, or subtracting the mean pointing errors for the two edges. Three examples of different image shapes should clarify and illustrate the rules for computing the mean measurement error.

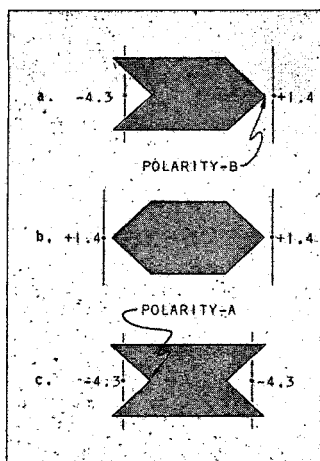


Figure 1A. Examples of hypothetical images. The dot on the line shows the location of the mean error relative to the edge. The number next to each line is the mean pointing error in microns.

Figure 1A shows three representations of hypothetical images. The edges of each "image" are 90 degree angles. Example a is formed by a polarity-A and a polarity-B edge, example b is formed by two polarity-B edges, and example c is formed by two polarity-A edges. Assume the edge spread is 16.8 microns. The dot on the vertical line indicates the position of the mean error relative to the edge, and the number above the line is the mean pointing error in microns. (The numbers were taken from Table 1A.)

To compute the mean measurement error for example a, subtract the mean pointing error of -4.3 from $+1.4$. The mean measurement error to be expected is $+5.7$ microns when operators measure this kind of image with an edge spread of 16.8 microns. That is, this image will be measured about 6 microns longer than its true length. This example illustrates the first rule. If the signs of the means of the pointing errors for the two edges are different and (1) each mean is outside the image, subtract the negative mean from the positive mean (2) each mean is inside the image, subtract the positive mean from the negative mean.

To compute the mean measurement error for example b, add the pointing errors of $+1.4$ and $+1.4$. The mean measurement error expected for this image would be $+2.8$ microns. This example illustrates the second rule. If a positive mean for each edge indicates each mean is outside the image, or if a negative mean for each edge indicates each mean is inside the image, add the two means.

To compute the mean measurement error for example c, add the pointing errors and change the sign of the sum. The mean measurement error for this image would be $+8.6$ microns. This example illustrates the third rule. If a negative mean for each edge indicates each mean is outside the image, or if a positive mean for each edge indicates each mean is inside the image, add the two means and change the sign of the sum.

The Standard Deviation of Measurement Errors

Tables 2A through 20A show the standard deviations and the variances of the pointing errors for each edge at the different combinations of edge spreads and modulations.

TABLES 2A through 20A

Each of the following tables shows the standard deviations (s) and variances (s^2) of the pointing errors for the different edges for one combination of edge spread and modulation. The numbers in the body of the tables are correlation coefficients.

TABLE 2A
EDGE SPREAD-5.0 MICRONS
MODULATION-.10

			POLARITY-A POINTED EDGES (ANGLES)				POLARITY-A CURVED EDGE	POLARITY-B POINTED EDGES (ANGLES)				POLARITY-B CURVED/ STRAIGHT EDGE
			135°	90°	45°	22°		135°	90°	45°	22°	
			s	s^2								
POLARITY-A POINTED EDGES (ANGLES)		s	4.5	20.02	.77							
		s^2	20.02	35.61	35.92	224.31	12.78	18.52	50.98	63.99	124.02	19.90
	135°	4.5	20.02	.77								
	90°	6.0	35.61	.90	.57							
	45°	6.0	35.92	.45	.19	.85						
POLARITY-A CURVED EDGE	22°	14.9	224.31	.58	.28	.65	.67					
		3.6	12.78	.97	.93	.48	.54	.74				
	135°	4.3	18.52	.49	.25	.62	.94	.53	.80			
	90°	7.1	50.98	.24	-.03	.61	.92	.25	.93	.88		
	45°	8.0	63.99	.54	.42	.47	.82	.63	.95	.80	.46	
POLARITY-B POINTED EDGES (ANGLES)	22°	11.1	124.02	.68	.51	.20	.83	.64	.81	.66	.82	.41
		4.5	19.90	.71	.42	.40	.79	.65	.76	.57	.70	.85
POLARITY-B CURVED/STRAIGHT EDGE												.64

TABLE 3A
EDGE SPREAD-7.5 MICRONS
MODULATION-.10

			POLARITY-A POINTED EDGES (ANGLES)				POLARITY-A CURVED EDGE	POLARITY-B POINTED EDGES (ANGLES)				POLARITY-B CURVED/ STRAIGHT EDGE
			135°	90°	45°	22°		135°	90°	45°	22°	
			s	s^2								
POLARITY-A POINTED EDGES (ANGLES)		s	6.6	43.23	-.17							
		s^2	43.23	41.60	42.41	36.98	14.46	61.05	8.76	28.41	394.36	27.86
	135°	6.6	43.23	-.17								
	90°	6.4	41.60	-.80	.32							
	45°	6.5	42.41	-.47	.79	.09						
POLARITY-A CURVED EDGE	22°	6.1	36.98	-.48	-.01	.09	.06					
		3.8	14.46	.55	-.81	-.50	.32	.13				
	135°	7.8	61.05	-.35	.30	.48	.52	-.34	.66			
	90°	3.0	8.76	-.03	-.29	-.19	.57	.06	.76	.23		
	45°	5.3	28.41	-.64	.31	.13	.61	-.42	.79	.77	.40	
POLARITY-B POINTED EDGES (ANGLES)	22°	19.9	394.36	-.44	-.05	-.33	.54	-.18	.46	.75	.87	.64
		5.3	27.86	.06	.13	.61	.26	-.12	.82	.50	.32	-.06
POLARITY-B CURVED/STRAIGHT EDGE												.47

TABLE 4A
EDGE SPREAD-11.2 MICRONS
MODULATION-.10

			POLARITY-A POINTED EDGES (ANGLES)				POLARITY-A CURVED EDGE	POLARITY-B POINTED EDGES (ANGLES)				POLARITY-B CURVED/ STRAIGHT EDGE		
			135°	90°	45°	22°		135°	90°	45°	22°			
			S											
			S	S2	7.1	4.9	10.9	10.4	4.9	7.4	8.4	4.9	8.8	4.1
			S	S2	49.97	24.04	117.99	108.41	24.31	55.03	70.10	24.17	77.54	17.11
POLARITY-A POINTED EDGES (ANGLES)	135°	7.1	49.97	-.43										
	90°	4.9	24.04	.19	.44									
	45°	10.9	117.99	.50	.78	.49								
	22°	10.4	108.41	.07	.80	.78	.27							
POLARITY-A CURVED EDGE			4.9	24.31	-.13	-.18	-.23	.24	.62					
POLARITY-B POINTED EDGES (ANGLES)	135°	7.4	55.03	.24	-.42	-.62	-.52	.42	.55					
	90°	8.4	70.10	.42	-.24	-.36	-.30	.23	.83	.55				
	45°	4.9	24.17	-.15	.43	.13	.14	-.60	-.25	.15	.38			
	22°	8.8	77.54	-.55	-.56	-.86	-.41	.46	.57	.49	.06	.01		
POLARITY-B CURVED/STRAIGHT EDGE			4.1	17.11	.08	-.21	-.55	-.24	.57	.92	.84	-.07	.68	.56

TABLE 5A
EDGE SPREAD-16.8 MICRONS
MODULATION-.10

				POLARITY-A POINTED EDGES (ANGLES)				POLARITY-A CURVED EDGE	POLARITY-B POINTED EDGES (ANGLES)				POLARITY-B CURVED/ STRAIGHT EDGE
				135°	90°	45°	22°		135°	90°	45°	22°	
				S									
		S	S2	117.50	120.39	267.68	323.41	57.64	48.99	51.10	124.75	764.24	36.62
POLARITY-A POINTED EDGES (ANGLES)	135°	11.7	137.50	.75									
	90°	11.0	120.39	.26	.03								
	45°	16.4	267.68	.68	.86	.36							
	22°	18.0	323.41	.14	.88	.76	.37						
POLARITY-A CURVED EDGE		7.6	57.64	.70	.13	.55	.29	.26					
POLARITY-B POINTED EDGES (ANGLES)	135°	7.0	48.99	.50	-.57	-.22	-.67	.22	.29				
	90°	7.1	51.10	.35	-.34	-.02	-.52	.39	.43	.11			
	45°	11.2	124.75	.75	-.37	.06	-.51	.41	.94	.51	.04		
	22°	27.6	764.24	.73	-.37	.09	-.48	.55	.91	.64	.96	.76	
POLARITY-B CURVED/STRAIGHT EDGE		6.1	36.62	.00	-.46	-.28	-.03	.41	.20	-.23	.13	.14	.11

TABLE 6A
EDGE SPREAD-7.5 MICRONS
MODULATION-.15

				POLARITY-A POINTED EDGES (ANGLES)				POLARITY-A CURVED EDGE	POLARITY-B POINTED EDGES (ANGLES)				POLARITY-B CURVED/ STRAIGHT EDGE
				135°	90°	45°	22°		135°	90°	45°	22°	
				S									
		S	S2	10.45	54.79	43.58	106.44	11.30	11.34	19.22	26.39	60.25	15.82
POLARITY-A POINTED EDGES (ANGLES)	135°	3.2	10.45	.41									
	90°	7.4	54.79	.04	.30								
	45°	6.6	43.58	-.28	.22	.47							
	22°	10.3	106.44	-.23	.52	.88	.60						
POLARITY-A CURVED EDGE		3.4	11.30	.77	-.39	-.07	-.08	.70					
POLARITY-B POINTED EDGES (ANGLES)	135°	3.4	11.34	-.15	-.77	.38	-.04	.25	.70				
	90°	4.4	19.22	-.26	-.43	.53	.24	.09	.82	.75			
	45°	5.1	26.39	-.73	-.03	.44	.28	-.58	.40	.74	-.03		
	22°	7.8	60.25	-.36	.34	.51	.29	-.65	.13	.13	.41	-.10	
POLARITY-B CURVED/STRAIGHT EDGE		4.0	15.82	-.19	-.78	.35	.01	.31	.96	.88	.47	-.07	.77

TABLE 7A
EDGE SPREAD-24.0 MICRONS
MODULATION-.15

				POLARITY-A POINTED EDGES (ANGLES)				POLARITY-A CURVED EDGE	POLARITY-B POINTED EDGES (ANGLES)				POLARITY-B CURVED/ STRAIGHT EDGE		
				135°	90°	45°	22°		135°	90°	45°	22°			
				S	7.1	7.3	16.0	19.0	8.0	4.4	8.5	16.1	17.4	8.5	
				S	S2	50.3	52.77	256.73	360.63	63.78	19.50	72.33	258.33	303.81	72.13
POLARITY-A POINTED EDGES (ANGLES)	135°	7.1	50.3	.29											
	90°	7.3	52.77	.90	.50										
	45°	16.0	256.73	.44	.36	.72									
	22°	19.0	360.63	.89	.84	.21	.42								
POLARITY-A CURVED EDGE		8.0	63.78	.88	.60	.36	.78	.71							
POLARITY-B POINTED EDGES (ANGLES)	135°	4.4	19.50	-.70	-.52	-.64	-.74	-.72	.76						
	90°	8.5	72.33	.04	.26	-.34	.41	-.18	-.01	-.01					
	45°	16.1	258.33	-.29	-.35	.59	-.23	-.22	-.36	-.02	.20				
	22°	17.4	303.81	-.65	-.70	.32	-.64	-.51	.10	-.17	.88	.73			
POLARITY-B CURVED/STRAIGHT EDGE		8.5	72.13	.33	.41	-.58	.64	.24	-.08	.79	-.53	-.67	.16		

TABLE 8A
EDGE SPREAD-7.5 MICRONS
MODULATION-.22

			POLARITY-A POINTED EDGES (ANGLES)				POLARITY-A CURVED EDGE	POLARITY-B POINTED EDGES (ANGLES)				POLARITY-B CURVED/ STRAIGHT EDGE		
			135°	90°	45°	22°		135°	90°	45°	22°			
			S	3.8	4.4	4.3	6.2	2.2	3.3	2.9	3.8	3.8	2.0	
			S	S ²	14.60	19.04	18.36	38.23	4.67	10.62	8.36	14.57	14.54	4.21
POLARITY-A POINTED EDGES (ANGLES)	135°	3.8	14.60	.67										
	90°	4.4	19.04	.28	.20									
	45°	4.3	18.36	.24	.96	.85								
	22°	6.2	38.23	.27	.80	.82	.79							
POLARITY-A CURVED EDGE		2.2	4.67	.66	.43	.39	.04	.45						
POLARITY-B POINTED EDGES (ANGLES)	135°	3.3	10.62	.77	.21	.20	-.06	.94	.52					
	90°	2.9	8.36	.46	-.10	-.03	-.37	.80	.89	.08				
	45°	3.8	14.57	.57	.05	.11	-.27	.88	.94	.97	.82			
	22°	3.8	14.54	-.14	.80	.74	.37	.43	.12	.01	.12	.28		
POLARITY-B CURVED/STRAIGHT EDGE		2.0	4.21	.23	-.49	-.59	-.83	.44	.50	.60	.58	-.20	.77	

TABLE 9A
EDGE SPREAD-11.2 MICRONS
MODULATION-.22

			POLARITY-A POINTED EDGES (ANGLES)				POLARITY-A CURVED EDGE	POLARITY-B POINTED EDGES (ANGLES)				POLARITY-B CURVED/ STRAIGHT EDGE		
			135°	90°	45°	22°		135°	90°	45°	22°			
			S	2.5	2.0	4.9	4.6	2.9	3.7	3.8	4.0	5.1	3.6	
			S	S2	6.25	3.97	23.63	21.35	8.66	13.95	14.11	16.39	25.88	12.65
POLARITY-A POINTED EDGES (ANGLES)	135°	2.5	6.25	-.40										
	90°	2.0	3.97	-.10	.26									
	45°	4.9	23.63	.42	-.52	-.22								
	22°	4.6	21.35	.11	.52	.39	.57							
POLARITY-A CURVED EDGE		2.9	8.66	.20	.77	-.73	.02	.68						
POLARITY-B POINTED EDGES (ANGLES)	135°	3.7	13.95	-.11	.62	-.85	-.17	.80	.58					
	90°	3.8	14.11	.21	-.05	.27	.01	-.20	.10	.35				
	45°	4.0	16.39	.26	.25	-.72	-.49	.77	.80	-.11	.58			
	22°	5.1	25.88	.20	.00	-.67	-.69	.61	.61	-.27	.94	.63		
POLARITY-B CURVED/STRAIGHT EDGE		3.6	12.65	-.26	.58	-.98	-.31	.84	.85	-.35	.79	.73	.45	

TABLE 10A
EDGE SPREAD-16.8 MICRONS
MODULATION-.22

			POLARITY-A POINTED EDGES (ANGLES)				POLARITY-A CURVED EDGE	POLARITY-B POINTED EDGES (ANGLES)				POLARITY-B CURVED/ STRAIGHT EDGE		
			135°	90°	45°	22°		135°	90°	45°	22°			
			S	5.4	5.4	8.3	9.7	3.7	1.9	4.5	5.8	15.1	2.2	
S			S2	28.68	29.55	68.23	93.89	13.34	3.62	20.05	33.80	226.65	4.65	
POLARITY-A POINTED EDGES (ANGLES)	135°	5.4	28.68	.78										
	90°	5.4	29.55	.77	.56									
	45°	8.3	68.23	.60	.90	.30								
	22°	9.7	93.89	.70	.79	.62	.79							
POLARITY-A CURVED EDGE			3.7	13.34	.75	.63	.53	.18	.46					
POLARITY-B POINTED EDGES (ANGLES)	135°	1.9	3.62	-.79	-.75	-.64	-.39	-.90	.53					
	90°	4.5	20.05	-.65	-.48	-.27	-.39	-.57	.82	.45				
	45°	5.8	33.80	-.69	-.27	-.33	-.08	-.69	.71	.61	-.24			
	22°	15.1	226.65	-.65	-.45	-.17	-.42	-.53	.77	.98	.53	.79		
POLARITY-B CURVED/STRAIGHT EDGE			2.2	4.65	.08	-.17	-.37	-.50	.55	-.36	-.34	-.28	-.37	.41

TABLE 11A
EDGE SPREAD-24.0 MICRONS
MODULATION-.22

				POLARITY-A POINTED EDGES (ANGLES)				POLARITY-A CURVED EDGE	POLARITY-B POINTED EDGES (ANGLES)				POLARITY-B CURVED/ STRAIGHT EDGE		
				135°	90°	45°	22°		135°	90°	45°	22°			
				S	6.6	8.7	13.1	18.1	6.4	6.1	7.5	13.5	20.3	5.1	
				S	S ²	44.30	76.04	170.78	329.37	40.69	37.37	56.15	182.04	412.17	26.15
POLARITY-A POINTED EDGES (ANGLES)	135°	6.6	44.30	.27											
	90°	8.7	76.04	.86	.62										
	45°	13.1	170.78	.54	.75	.56									
	22°	18.1	329.37	.39	.28	.72	.78								
POLARITY-A CURVED EDGE			6.4	40.69	.67	.55	.38	.36	.53						
POLARITY-B POINTED EDGES (ANGLES)	135°	6.1	37.37	-.68	-.24	.12	-.14	-.34	.78						
	90°	7.5	56.15	.07	.19	-.08	-.34	.63	.24	.46					
	45°	13.5	182.04	-.03	.16	-.31	-.73	.24	.23	.85	.90				
	22°	20.3	412.17	.39	.29	-.16	-.18	.43	-.24	.54	.59	.43			
POLARITY-B CURVED/STRAIGHT EDGE			5.1	26.15	.13	.36	.11	-.23	.36	.36	.75	.76	.77	.16	

TABLE 12A
EDGE SPREAD-5.0 MICRONS
MODULATION-.33

				POLARITY-A POINTED EDGES (ANGLES)				POLARITY-A CURVED EDGE	POLARITY-B POINTED EDGES (ANGLES)				POLARITY- CURVED/ STRAIGHT EDGE		
				135°	90°	45°	22°		135°	90°	45°	22°			
				S	2.4	2.1	4.8	5.1	1.9	2.6	3.4	3.5	5.5	2.6	
				S	S2	5.62	4.39	22.50	26.40	3.49	6.68	11.40	12.58	30.72	6.83
POLARITY-A POINTED EDGES (ANGLES)	135°	2.4	5.62	.23											
	90°	2.1	4.39	.86	.53										
	45°	4.8	22.50	.58	.74	.28									
	22°	5.1	26.40	.72	.97	.80	.35								
POLARITY-A CURVED EDGE				1.9	3.49	.62	.86	.71	.85	.56					
POLARITY-B POINTED EDGES (ANGLES)	135°	2.6	6.68	.16	.56	.37	.66	.68	.46						
	90°	3.4	11.40	.64	.85	.44	.83	.80	.84	.73					
	45°	3.5	12.58	.82	.92	.76	.88	.94	.59	.84	.67				
	22°	5.5	30.72	.52	.81	.68	.85	.90	.89	.90	.89	.80			
POLARITY-B CURVED/STRAIGHT EDGE				2.6	6.83	.92	.68	.42	.52	.54	.17	.62	.77	.51	.84

TABLE 13A
EDGE SPREAD-7.5 MICRONS
MODULATION-.33

		POLARITY-A POINTED EDGES (ANGLES)				POLARITY-A CURVED EDGE	POLARITY-B POINTED EDGES (ANGLES)				POLARITY-B CURVED/ STRAIGHT EDGE
		135°	90°	45°	22°		135°	90°	45°	22°	
		S	S	S	S		S	S	S	S	
POLARITY-A POINTED EDGES (ANGLES)	S	S	S	S	S		S	S	S	S	
	S	S	S	S	S		S	S	S	S	
	S	S	S	S	S		S	S	S	S	
	S	S	S	S	S		S	S	S	S	
	S	S	S	S	S		S	S	S	S	
POLARITY-A CURVED EDGE		2.0	3.85	.82	.98	.80	.93	.74			
POLARITY-B POINTED EDGES (ANGLES)	135°	1.7	3.01	.30	.47	.73	.53	.33	.52		
	90°	3.0	9.22	.25	.24	.61	.42	.16	.83	.69	
	45°	5.7	32.38	.08	.07	.48	.24	.00	.76	.98	.77
	22°	6.1	37.75	-.11	-.09	.36	.07	-.18	.74	.92	.97
	22°	6.1	37.75	-.11	-.09	.36	.07	-.18	.74	.92	.97
POLARITY-B CURVED/STRAIGHT EDGE		1.6	2.61	.68	.92	.97	.96	.87	.72	.52	.36

TABLE 14A
EDGE SPREAD-11.2 MICRONS
MODULATION-.33

		POLARITY-A POINTED EDGES (ANGLES)				POLARITY-A CURVED EDGE	POLARITY-B POINTED EDGES (ANGLES)				POLARITY-B CURVED/ STRAIGHT EDGE
		135°	90°	45°	22°		135°	90°	45°	22°	
		S	S	S	S		S	S	S	S	
POLARITY-A POINTED EDGES (ANGLES)	S	S	S	S	S		S	S	S	S	
	S	S	S	S	S		S	S	S	S	
	S	S	S	S	S		S	S	S	S	
	S	S	S	S	S		S	S	S	S	
	S	S	S	S	S		S	S	S	S	
POLARITY-A CURVED EDGE		2.7	7.40	.79	.52	.17	.00	.72			
POLARITY-B POINTED EDGES (ANGLES)	135°	3.3	10.95	.16	.26	.19	-.03	.52	.54		
	90°	4.2	17.41	.33	.38	.01	-.03	.59	.84	.72	
	45°	6.2	38.83	.05	.35	.19	.08	.27	.88	.86	.68
	22°	6.4	40.91	.47	.79	.54	.48	.39	.57	.66	.78
	22°	6.4	40.91	.47	.79	.54	.48	.39	.57	.66	.78
POLARITY-B CURVED/STRAIGHT EDGE		2.8	7.70	.43	.27	-.20	.32	.81	.67	.86	.60

TABLE 15A
EDGE SPREAD-16.8 MICRONS
MODULATION-.33

		POLARITY-A POINTED EDGES (ANGLES)				POLARITY-A CURVED EDGE	POLARITY-B POINTED EDGES (ANGLES)				POLARITY-B CURVED/ STRAIGHT EDGE
		135°	90°	45°	22°		135°	90°	45°	22°	
		S	S	S	S		S	S	S	S	
POLARITY-A POINTED EDGES (ANGLES)	S	S	S	S	S		S	S	S	S	
	S	S	S	S	S		S	S	S	S	
	S	S	S	S	S		S	S	S	S	
	S	S	S	S	S		S	S	S	S	
	S	S	S	S	S		S	S	S	S	
POLARITY-A CURVED EDGE		2.2	4.70	.72	.60	.67	.59	.46			
POLARITY-B POINTED EDGES (ANGLES)	135°	5.4	29.30	-.13	-.20	.63	.75	.03	.70		
	90°	5.2	26.77	.22	-.20	.70	.85	.23	.92	.84	
	45°	5.4	29.46	.14	-.65	-.21	.07	-.45	.42	.51	.83
	22°	15.5	239.68	.08	.89	.07	-.38	.22	-.31	-.35	-.40
	22°	15.5	239.68	.08	.89	.07	-.38	.22	-.31	-.35	-.40
POLARITY-B CURVED/STRAIGHT EDGE		2.9	8.36	.50	.20	.07	.20	.35	.28	.34	.33

TABLE 16A
EDGE SPREAD-24.0 MICRONS
MODULATION-.33

				POLARITY-A POINTED EDGES (ANGLES)				POLARITY-A CURVED EDGE	POLARITY-B POINTED EDGES (ANGLES)				POLARITY-B CURVED/ STRAIGHT EDGE		
				135°	90°	45°	22°		135°	90°	45°	22°			
				S	4.2	5.5	9.0	18.9	4.4	4.6	7.4	11.8	20.5	4.7	
				S	S ²	17.66	30.22	80.55	355.41	19.50	22.01	54.05	139.99	420.02	22.34
POLARITY-A POINTED EDGES (ANGLES)	135°	4.2	17.66	.35											
	90°	5.5	30.22	.86	.36										
	45°	9.0	80.55	.56	.50	.33									
	22°	18.9	355.41	.53	.66	.66	.77								
POLARITY-A CURVED EDGE				4.4	19.50	.53	.20	.13	-.40	.40					
POLARITY-B POINTED EDGES (ANGLES)	135°	4.6	22.01	-.75	-.80	-.87	-.90	.02	.14						
	90°	7.4	54.05	.06	.31	-.26	-.36	.28	.17	.32					
	45°	11.8	139.99	-.29	.11	-.45	-.28	-.20	.30	.87	.47				
	22°	20.5	420.02	.00	.33	-.52	-.14	-.06	.18	.60	.69	-.01			
POLARITY-B CURVED/STRAIGHT EDGE				4.7	22.34	-.07	-.14	-.50	-.01	-.16	.24	-.47	-.31	.35	.24

TABLE 17A
EDGE SPREAD-5.0 MICRONS
MODULATION-.50

				POLARITY-A POINTED EDGES (ANGLES)				POLARITY-A CURVED EDGE	POLARITY-B POINTED EDGES (ANGLES)				POLARITY-B CURVED/ STRAIGHT EDGE		
				135°	90°	45°	22°		135°	90°	45°	22°			
				S	2.4	2.8	3.1	7.3	1.6	2.6	3.3	3.3	4.3	1.2	
				S	S2	5.55	7.79	9.65	53.84	2.69	6.85	10.96	10.59	18.31	1.38
POLARITY-A POINTED EDGES (ANGLES)	135°	2.4	5.55	.36											
	90°	2.8	7.79	.91	.81										
	45°	3.1	9.65	.72	.92	.90									
	22°	7.3	53.84	.66	.81	.80	.86								
POLARITY-A CURVED EDGE			1.6	2.69	.78	.93	.96	.87	.75						
POLARITY-B POINTED EDGES (ANGLES)	135°	2.6	6.85	-.27	.10	.37	.36	.21	.38						
	90°	3.3	10.96	-.31	-.02	.27	.41	.18	.89	.73					
	45°	3.3	10.59	-.04	.28	.60	.55	.54	.78	.86	.84				
	22°	4.3	18.31	.20	.35	.62	.44	.59	.35	.53	.83	.76			
POLARITY-B CURVED/STRAIGHT EDGE			1.2	1.38	.77	.48	.18	.26	.36	-.79	-.72	-.52	-.16	.43	

TABLE 18A
EDGE SPREAD-7.5 MICRONS
MODULATION-.50

				POLARITY-A POINTED EDGES (ANGLES)				POLARITY-A CURVED EDGE	POLARITY-B POINTED EDGES (ANGLES)				POLARITY- CURVED/ STRAIGHT EDGE
				135°	90°	45°	22°		135°	90°	45°	22°	
				S	S	S2	2.3	2.1	4.4	4.1	2.9	4.0	4.1
		S	S2	5.09	4.45	19.45	16.96	8.41	15.69	16.54	28.50	45.66	6.84
POLARITY-A POINTED EDGES (ANGLES)	135°	2.3	5.09	.15									
	90°	2.1	4.45	.84	.48								
	45°	4.4	19.45	.62	.59	.27							
	22°	4.1	16.96	.80	.61	.87	.47						
POLARITY-A CURVED EDGE		2.9	8.41	.43	.70	.76	.61	.85					
POLARITY-B POINTED EDGES (ANGLES)	135°	4.0	15.69	.58	.65	.54	.75	.72	.80				
	90°	4.1	16.54	.39	.53	.52	.65	.81	.95	.92			
	45°	5.3	28.50	.34	.32	.54	.71	.70	.86	.94	.74		
	22°	6.8	45.66	.54	.46	.65	.85	.69	.91	.92	.97	.22	
POLARITY-B CURVED/STRAIGHT EDGE		2.6	6.84	.43	.57	.48	.60	.83	.90	.97	.91	.88	.81

TABLE 19A
EDGE SPREAD-11.2 MICRONS
MODULATION-.50

		POLARITY-A POINTED EDGES (ANGLES)				POLARITY-A CURVED EDGE	POLARITY-B POINTED EDGES (ANGLES)				POLARITY-B CURVED/ STRAIGHT EDGE
		135°	90°	45°	22°		135°	90°	45°	22°	
		S	S ²								
POLARITY-A POINTED EDGES (ANGLES)	135°	3.7	13.38	.74							
	90°	2.9	8.69	.74	.67						
	45°	4.3	18.14	.91	.71	.49					
	22°	10.2	103.70	.73	.53	.93	.51				
POLARITY-A CURVED EDGE		1.8	3.26	.82	.50	.87	.90	.58			
POLARITY-B POINTED EDGES (ANGLES)	135°	3.0	9.26	.31	.51	.34	.49	.56	.73		
	90°	2.7	7.05	.04	.50	.11	.23	.24	.91	.80	
	45°	4.2	17.45	-.07	.26	.11	.35	.35	.87	.91	.57
	22°	7.9	62.40	-.19	.01	.00	.30	.31	.81	.80	.96
POLARITY-B CURVED/STRAIGHT EDGE		1.6	2.69	.24	.60	.32	.09	-.14	-.25	-.04	-.23

TABLE 20A
EDGE SPREAD-25.0 MICRONS
MODULATION-.50

		POLARITY-A POINTED EDGES (ANGLES)				POLARITY-A CURVED EDGE	POLARITY-B POINTED EDGES (ANGLES)				POLARITY-B CURVED/ STRAIGHT EDGE
		135°	90°	45°	22°		135°	90°	45°	22°	
		S	S ²								
POLARITY-A POINTED EDGES (ANGLES)	135°	6.9	47.61	.16							
	90°	4.2	17.53	.72	-.03						
	45°	11.8	139.36	.38	.83	.38					
	22°	17.2	296.90	.91	.72	.45	.41				
POLARITY-A CURVED EDGE		3.7	13.58	.71	.57	.41	.56	.07			
POLARITY-B POINTED EDGES (ANGLES)	135°	5.9	35.20	-.88	-.94	-.75	-.87	-.61	-.05		
	90°	6.7	45.65	-.11	-.35	-.48	-.04	-.74	.21	.18	
	45°	11.1	122.57	.01	-.22	-.18	.13	-.63	.02	.88	.55
	22°	17.4	301.83	.20	-.11	-.13	.37	-.45	-.13	.81	.96
POLARITY-B CURVED/STRAIGHT EDGE		4.6	21.66	-.83	-.84	-.80	-.85	-.66	.94	.32	.00

The numbers in the body of each table are correlation coefficients (Pearson r's). In this context the correlation coefficient is an index of how much the operators' pointing errors on one edge covaried with their pointing errors on another edge. (A correlation can vary between -1.00 and +1.00).

The standard deviation (S), variance (S^2), and the correlation coefficient (r) are the statistics needed for computing the standard deviation (S_i) of the measurement errors for an image. The formula for computing S_i is

$$S_i = \sqrt{S_1^2 + S_2^2 \pm 2rS_1S_2}$$

where,

S_i = the standard deviation of the measurement errors for an image

S_1 and S_2 = the standard deviations of the pointing errors for the two edges

S_1^2 and S_2^2 = the variances of the pointing errors for the two edges

r = the correlation between the operators' pointing errors on the two edges.

Whether the quantity $2rS_1S_2$ is added to or subtracted from $S_1^2 + S_2^2$ can be determined from the rules for computing the mean measurement error. If the mean measurement error is obtained by subtraction (the first rule in the previous section), subtract $2rS_1S_2$. If the mean measurement error is obtained by addition (the second and third rules), add $2rS_1S_2$ to $S_1^2 + S_2^2$.

The following examples should clarify how S_i is computed. Assume an S_i is to be computed for each of the images shown in Figure 1A and that the modulation is .33 and the edge spread is 16.8 microns. Now, refer to Table 15A to obtain the values needed for computing S_i .

To compute S_i for example a in Figure 1A, first locate in Table 15A the column labeled polarity-A 90° (left edge of the image) and the row labeled polarity-B 90° (right edge of the image). The standard deviation and variance for each edge are given below the edge designation in the column and to the right of the edge designation in the row. In this example the standard deviations are 2.9 and 5.2 microns, the variances 8.60 and 26.77 microns, and correlation is -.20.

To compute S_i in this example, subtract $2rS_1S_2$ from $S_1^2 + S_2^2$, because the mean measurement error was obtained by subtraction. The solution for S_i is

$$\begin{aligned} S_i &= \sqrt{8.60 + 26.77 - 2(-.20)(2.9)(5.2)} \\ &= \sqrt{35.37 + 6.03} \\ &= 6.4 \end{aligned}$$

A standard deviation of 6.4 indicates that about two-thirds of the operators' measurements will lie between ± 6.4 microns of the mean measurement error. The mean measurement error for this

example was +5.7 microns, that is, the length of this image was overestimated by 5.7 microns. Consequently, the measurements of two-thirds of the operators should lie between -0.7 microns (5.7 microns - 6.4 microns) and +12.1 microns (5.7 + 6.4 microns) of the true length of this image.

To compute S_i for example b, locate the column and the row labeled "polarity-B 90°." Because this image is formed by identical edges, the standard deviation for each edge is 5.2 microns, the variance for each edge is 26.77 microns, and the correlation is .84.

To compute S_i in this example, add $2rS_1S_2$ to $S_1^2 + S_2^2$ because the mean measurement error was obtained by addition. The solution for S_i is

$$\begin{aligned} S_i &= \sqrt{26.77 + 26.77 + 2 (.84) (5.2) (5.2)} \\ &= \sqrt{53.44 + 48.13} \\ &= 10.1 \end{aligned}$$

The mean measurement error for this example was +2.8 microns. Consequently, the measurements of two-thirds of the operators should lie between -7.8 microns and +12.9 microns of the true length of this image.

To compute S_i for example c, locate the column and the row labeled "polarity-A 90°." Again, the image is formed by identical edges. The standard deviation and variance for each edge are 2.9 microns and 8.60 microns respectively, and the correlation is .71.

To compute S_i in this example, add $2rS_1S_2$ to $S_1^2 + S_2^2$ because the mean measurement error was obtained by addition. The solution for S_i is

$$\begin{aligned} S_i &= \sqrt{8.60 + 8.60 + 2 (.71) (2.9) (2.9)} \\ &= \sqrt{17.20 + 11.90} \\ &= 5.4 \end{aligned}$$

The mean measurement error for this example was -8.6 microns. Consequently, the measurements of two-thirds of the operators should lie between -14.0 microns and +3.2 microns of the true length of the image.

Two points should be reemphasized in interpreting the data described in this section. First, the data apply only to edges whose edge spreads do not overlap. Second, in this experiment the means and the standard deviations are statistics based on a small number of observations (six operators); therefore, they may vary substantially from one sample of operators to the next. (The amount of variation to be expected may be calculated from formulas given in most statistics books.) Consequently, these statistics should be interpreted as approximations of the true (population) values.

APPENDIX B

PREPARATION OF THE STIMULI

The array of shapes portrayed in Figure 1 on page 10 was produced in a large format. The geometric shapes were scribed in a Rubylith scribing material, using precision instruments. A greatly reduced copy of the format was then produced on Kodak High-Resolution Plate. This plate is referred to as the "master plate."

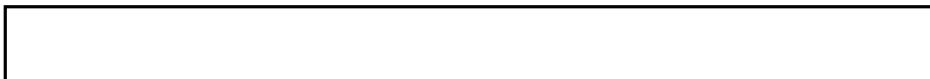
The master plate was used to produce a series of 19 photographic transparencies, Gems. The Gems were made by reproducing the master plate on Kodak High-Definition Aerial Film, Type 3404, which was then contact-printed onto Kodak Fine-Grain Aerial Duplicating Film, Type 8430. These two types of film were selected because they are used in many operational reconnaissance programs. The reproduction of the master plate onto Type 3404 film was such that its contact-print made on Type 8430 exhibited the desired image-structure characteristics.

The images on Type 3404 film were made using a modified contact-printing procedure described by With this technique, the master plate was separated from the Type 3404 film by a controlled distance using a thin sheet of glass as a spacer; the master plate-glass spacer-film sandwich was exposed a specific distance from a light source having an appropriate spatially varying intensity distribution. During exposure, the sandwich was held in a frame especially designed to allow the exposure given the area containing the geometric shapes to be different from the surrounding area containing the fiducial marks. The frame containing the sandwich was placed on a turntable whose center rotated normal to, and concentric with, a variable area mask covering the light source.

25X1

Using a pin-hole mask, the area on the Type 3404 film corresponding to the geometric shapes was given a uniform exposure without the master plate in position. This controlled exposure was made to yield the appropriate image modulation or contrast. The master plate was then positioned in the frame and with a pin-hole mask over the light source, the fiducial marks were exposed. The resulting fiducial mark images were sharp and of high-contrast. Then, with a Gaussian-shaped variable area mask over the light source, the area containing the geometric shapes was exposed. After exposure, the film

5X1



was processed in a tray in Kodak D-19 Developer for eight minutes at 20° C. Development was followed by the usual acetic-acid rinse, fixing, washing and drying. The characteristic curve for the processing of the Type 3404 film is shown in Figure 1B. The mean density of the images was 1.0, this being the mean density of most negative photographs produced in operational programs.

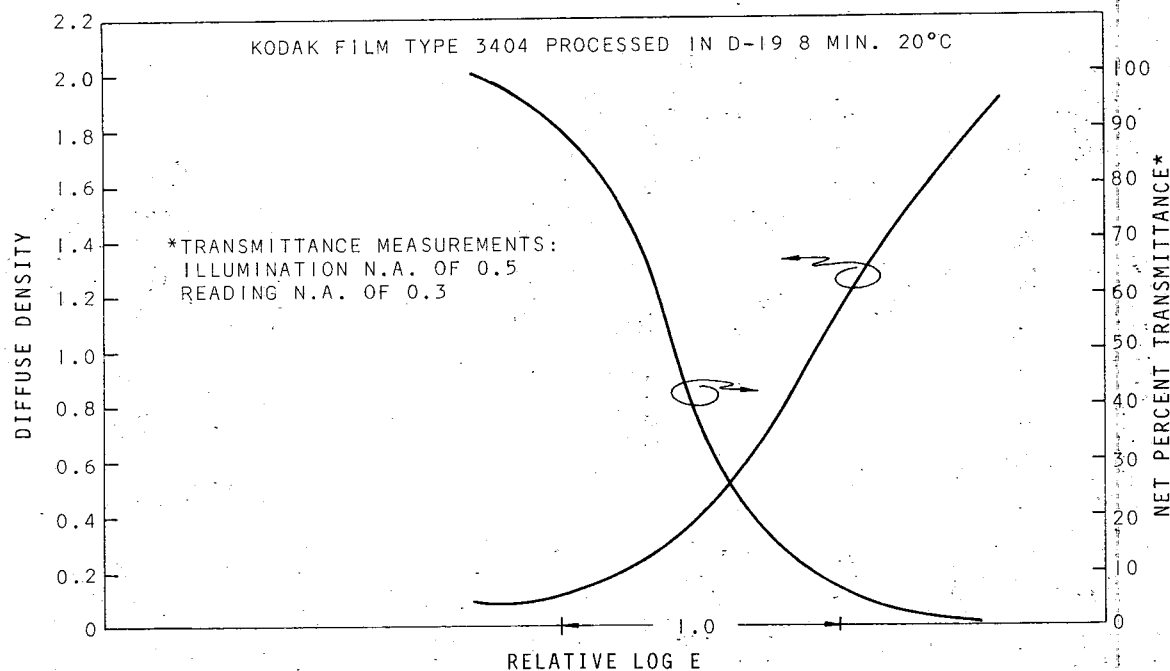


Figure 1B. Characteristic curves for Kodak Type 3404 film.

The images on Type 3404 film were contact-printed on Kodak Fine-Grain Aerial Duplicating Film, Type 8430, using a high-resolution contact printer. The mean density of the images on Type 8430 film was 1.0. The Type 8430 film was tray-processed in Kodak D-76 Developer for eight minutes at 20° C. The characteristic curve for the Type 8430 film images is shown in Figure 2B on the next page. The images on Type 8430 film are the transparencies referred to as Gems.

The long, straight edge between edges 35 and 16 (see Figure 1B above) of each Gem was scanned with a microdensitometer to assess the modulation and edge spread of the images. The Gems with a 5-micron edge spread were scanned with an illumination objective with a N.A. = 0.5, and a reading objective with a N.A. = 0.65, and with an effective slit width of 1.75 microns. All other Gems were scanned with an illumination objective with a N.A. = 0.5, a reading objective with a N.A. = 0.3, and an effective slit width of 3.5 microns.

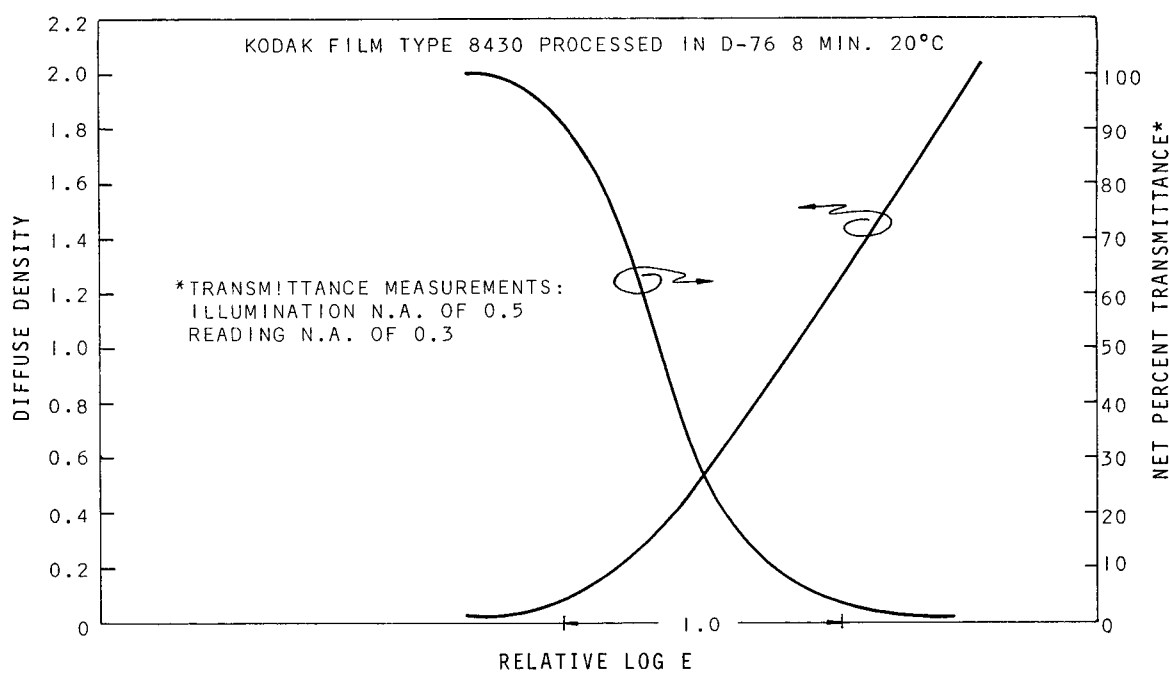


Figure 2B. Characteristic curves for Kodak Type 8430 film.

The microdensitometer was adjusted to read 100 percent transmittance on an unexposed portion of the film in making transmittance measurements. Thus, all the reported values are net transmittance or net density. The long, straight edge was scanned at three places along its length. Each scan sampled 800 microns of the length of the edge. The reported edge spread was determined by taking the average of the three scans made of each Gem; the averaging technique is discussed in the main body of the text, and is illustrated in Figure 4 on page 12.

The RMS granularity of the Gems was measured using conventional techniques and found to be 0.008, which is the value normally given for this film at a net density of 1.0 and for a scanning aperture 24 microns in diameter.

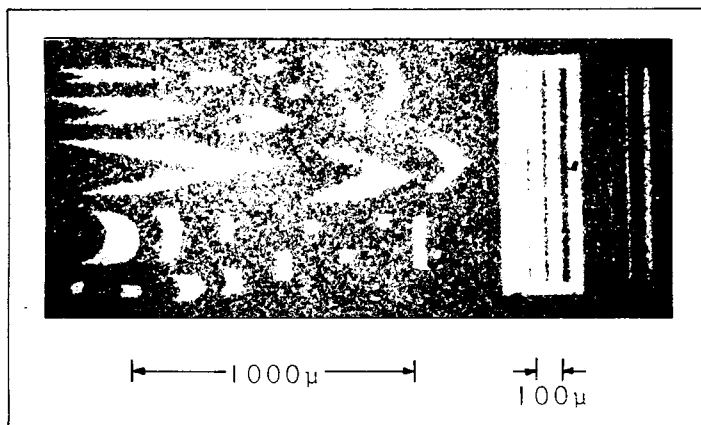


Figure 3B. Photomicrograph of Gem No. 12.

The Gems were mounted between two sheets of No. 2 (0.22 mm thick) microscope cover glass for abrasion protection and for handling convenience. A photomicrograph of Gem No. 12 is shown in Figure 3B.

Ellen pls file in

Pym

997114

May 26, 1965

Dear Dick:

Clearances sufficient to give a blue visitor badge to [redacted] are requested so that he can participate in photo-interpreter response studies being performed for, and in, [redacted] As with other contractors participating in this work, [redacted] needs more than one [redacted] representative for active participation in this work. [redacted] primary activity will be the administration of photo-interpreter tests and the preparation of testing materials. This effort requires that [redacted] work in the building for periods ranging from days to weeks, and his ability to move freely in the building will facilitate our efforts.

25X1

25X1
25X1

25X1

Regards,

[redacted signature box]